DIGITAL ACCESS TO SCHOLARSHIP AT HARVARD
DASH.HARVARD.EDU

HARVARD LIBRARY
Office for Scholarly Communication

Identification of spinal circuits involved in touch-evoked dynamic mechanical pain

The Harvard community has made this article openly available. **Please share** how this access benefits you. Your story matters

Citation	Cheng, L., B. Duan, T. Huang, Y. Zhang, Y. Chen, O. Britz, L. Garcia-Campmany, et al. 2017. "Identification of spinal circuits involved in touch-evoked dynamic mechanical pain." Nature neuroscience 20 (6): 804-814. doi:10.1038/nn.4549. http://dx.doi.org/10.1038/nn.4549.
Published Version	doi:10.1038/nn.4549
Citable link	http://nrs.harvard.edu/urn-3:HUL.InstRepos:34492288
Terms of Use	This article was downloaded from Harvard University's DASH repository, and is made available under the terms and conditions applicable to Other Posted Material, as set forth at http://nrs.harvard.edu/urn-3:HUL.InstRepos:dash.current.terms-of-use#LAA

Identification of spinal circuits involved in touch-evoked dynamic mechanical pain

Longzhen Cheng[1,2,*], **Bo Duan**[2,6,*], **Tianwen Huang**[2,*], **Yan Zhang**[2,3], **Yangyang Chen**[1], **Olivier Britz**[4], **Lidia Garcia-Campmany**[4], **Xiangyu Ren**[2,4], **Linh Vong**[5], **Bradford B. Lowell**[5], **Martyn Goulding**[4], **Yun Wang**[1,#], and **Qiufu Ma**[2,#]

[1]Institute of Brain Science, the State Key Laboratory of Medical Neurobiology and the Collaborative Innovation Center for Brain Science, Fudan University, Shanghai, China

[2]Dana-Farber Cancer Institute and Department of Neurobiology, Harvard Medical School, 1 Jimmy Fund Way, Boston, Massachusetts, USA

[3]Cell Electrophysiology Laboratory, Wannan Medical College, Wuhu, Anhui, China

[4]Molecular Neurobiology Laboratory, the Salk Institute for Biological Studies, 10010 North Torrey Pines Road, La Jolla, California, USA

[5]Division of Endocrinology, Diabetes, and Metabolism, Department of Medicine, Beth Israel Deaconess Medical Center, Harvard Medical School, 3 Blackfan Circle, Boston, Massachusetts, USA

Abstract

Mechanical hypersensitivity is a debilitating symptom associated with millions of chronic pain patients. It exists in distinct forms, including brush-evoked dynamic and filament-evoked punctate. Here we report that dynamic mechanical hypersensitivity induced by nerve injury or inflammation was compromised in mice with ablation of spinal VT3[Lbx1] neurons defined by coexpression of VGLUT3[Cre] and Lbx1[Flpo], as indicated by the loss of brush-evoked nocifensive responses and conditional place aversion. Electrophysiological recordings show that VT3[Lbx1] neurons form morphine-resistant polysynaptic pathways relaying inputs from low-threshold Aβ mechanoreceptors to lamina I output neurons. Meanwhile, the subset of somatostatin (SOM) lineage neurons preserved in VT3[Lbx1] neuron-ablated mice is largely sufficient to mediate von

Frey filament-evoked punctate mechanical hypersensitivity, including both morphine-sensitive and morphine-resistant forms. Furthermore, acute silencing of VT3[Lbx1] neurons attenuated pre-established dynamic mechanical hypersensitivity induced by nerve injury, suggesting these neurons as a potential cellular target for treating this form of neuropathic pain.

Introduction

Clinical observations showing pain can be evoked by innocuous mechanical stimuli, called mechanical allodynia, have contributed to the development of the gate control theory of pain[1–3]. According to this theory, spinal pain transmission neurons receive inputs from both nociceptors and low threshold mechanoreceptors (LTMRs), with LTMR inputs being gated by feedforward inhibition[3–8]. In chronic pain conditions caused by nerve lesions or inflammation, attenuation of this feedforward inhibition plus sensitization of primary and relay neurons opens the gate, allowing LTMR inputs to activate pain transmission neurons and allodynia manifestation to occur[9–12]. Allodynia exists in multiple forms in humans, including dynamic, static, and punctate. Dynamic allodynia, one of most bothersome and prevalent forms of chronic pain, is evoked by stimulation as gentle as skin touch by garments, running water, or even wind[13]. Static allodynia is evoked by pressure generated by a large probe (1-cm diameter in human studies)[14,15], which is probably equivalent to the Randall-Selitto assay used for animal studies. Punctate allodynia, wrongly termed "static" allodynia in animal studies[5,16,17], is evoked by von Frey filament stimulation. In human psychophysical studies, dynamic allodynia is associated with shooting, lancinating, burning and sore sensations, and static allodynia is of a burning quality[13–15,18,19]. Percepts associated with punctate allodynia may have not yet been carefully documented.

Several studies indicate different neural substrates mediating distinct forms of allodynia or mechanical hypersensitivity (in this study, allodynia means pain evoked by innocuous stimuli, whereas mechanical hypersensitivity is used to describe enhanced nocifensive motor behaviors in response to innocuous stimuli, without actual measurement of emotional/ cognitive aspects of pain). For primary afferents, myelinated LTMRs are required to mediate dynamic allodynia in humans[14,15,18–22], whereas unmyelinated C fibers can sufficiently transmit pressure-evoked static allodynia[14,15]. Animal studies show that punctate mechanical hypersensitivity may be transmitted via both A and C fibers[23–25]. However, it remains unknown if there are spinal circuits differentially involved in distinct forms of allodynia/mechanical hypersensitivity. Glycinergic neurons gate dynamic hypersensitivity at hindbrain levels[16], but also the punctate form at spinal levels[4,6]. Similarly, spinal interneurons expressing the gamma isoform of protein kinase C (PKCγ) might mediate both dynamic[16] and punctate[4,7,26] mechanical hypersensitivity. Spinal neurons marked by somatostatin[Cre] (SOM[Cre]) and spinal circuits whose maturation is influenced by transient developmental expression of the vesicular glutamate transporter 3 (VGLUT3) are involved with both forms of hypersensitivity as well[5,27].

Here we selectively ablated or silenced adult spinal neurons that are marked by co-expression of the Cre and Flpo DNA recombinases driven from the *Vglut3* gene locus (*VT3[Cre]*) and the *Lbx1* gene locus (*Lbx1[Flpo]*), respectively. We referred to these neurons as

VT3[Lbx1] neurons. Using behavioral and electrophysiological studies, we show that VT3[Lbx1] neurons form a morphine-resistant microcircuit necessary for the transmission of brush-evoked dynamic mechanical allodynia. We have further characterized multiple morphine-sensitive and morphine-resistant spinal circuits that are eliminated in SOM[Lbx1] neuron-ablated mice, but preserved in VT3[Lbx1] neuron-ablated mice, which could potentially mediate von Frey filament-evoked punctate hypersensitivity.

Results

Spinal neurons marked by VT3[Cre] expression

To mark VGLUT3 lineage neurons, we generated the *Vglut3-ires-Cre* (referred to as *VT3[Cre]*) mice, in which a cassette containing the *Cre* recombinase gene was inserted into the *Vglut3* (*Slc17a8*) gene locus, 3′ to the stop codon sequence (Supplementary Fig. 1a). By crossing *VT3[Cre]* mice with ai14 tdTomato reporter mice[28], spinal neurons that developmentally express VT3[Cre] were labeled with the red fluorescent tdTomato protein (Fig. 1a–c). At postnatal day 4 (P4), most neurons with detectable VGLUT3 mRNA (92%, 304/330) co-expressed tdTomato (Fig. 1a). The percentage of tdTomato^{+} neurons with detectable VGLUT3 mRNA declined from 34% (304/889) at P4, to 21% (288/1344) at P7, and to near none at adult stages, consistent with transient VGLUT3 expression[27]. We refer to VT3[Cre]-marked spinal neurons as VT3[Cre]-tdTomato[+].

We next performed double staining immunohistochemistry with lamina-specific markers. The neurokinin receptor (NK1R) marks a major subset of ascending projection neurons in lamina I[29]. VT3[Cre]-tdTomato^{+} neurons are located ventral to NK1R^{+} neurons with little overlap (2/195; Fig. 1b). They are intermingled with IB4^{+} terminals that label non-peptidergic primary afferent nociceptors that terminate in the dorsal lamina II inner layer ($_dII_i$)[28], and are also found in lamina II outer layer (II_o) that receives inputs from peptidergic nociceptor afferents (Fig. 1b)[29]. PKCγ[+] interneurons, which have been implicated in the transmission of neuropathic pain[4,7,26], are located in the ventral portion of lamina II inner layer ($_vII_i$) and in the most dorsal area of lamina III ($_dIII$), an area receiving inputs from LTMRs[30,31], which is referred to as the II-III border area (or $_vII_i$-$_dIII$). VT3[Cre]-tdTomato^{+} neurons were observed in both $_vII_i$-$_dIII$ and more ventral lamina III (Fig. 1b), and 42% (234/567) of PKCγ^{+} neurons coexpressed tdTomato. Thus, VT3[Cre]-tdTomato^{+} neurons are scattered throughout laminae II and III. The vast majority of adult VT3[Cre]-tdTomato^{+} neurons are excitatory, with 96% (540/563) expressing the vesicular glutamate transporter VGLUT2 (Fig. 1c), and only very few tdTomato^{+} cells express inhibitory neuron markers (Supplementary Fig. 1b). VT3[Cre]-tdTomato^{+} cells account for 32% (540/1671) of total VGLUT2^{+} glutamatergic neurons within laminae II and III (Fig. 1c).

Spinal neurons marked by SOM[Cre] transmit acute mechanical pain and mediate chronic mechanical hypersensitivity[5]. In $_vII_i$-$_dIII$, 38% (126/328) of VT3[Cre]-tdTomato^{+} neurons co-expressed SOM mRNA, and 28% (126/455) of SOM^{+} neurons coexpressed tdTomato (Supplementary Fig. 1c). Partial overlap between VT3[Cre]-tdTomato and SOM mRNA was also observed in I-II$_i$ and in III-IV, albeit to lower degrees than that in $_vII_i$-$_dIII$ (Supplementary Fig. 1c). We also found that 45% (369/827) of Calb2^{+} (Calretinin^{+}) cells are marked by VT3[Cre]-tdTomato (Supplementary Fig. 1d), indicating that spinal neurons

marked by our knock-in *VT3^Cre* are not identical to those marked by the transgenic *VT3::Cre*, which marks only 8% of adult Calb2+ neurons[27].

Impaired transmission of light punctate mechanical information following ablation of *VT3^Cre*-marked neurons

To assess the function of the VT3^Cre-derived neurons, we used an intersectional genetic strategy[5,32] to express the diphtheria toxin (DTX) receptor (DTR) in these neurons (Fig. 1d). To do this, *VT3^Cre* mice and *Lbx1^Flpo* mice[32] were crossed with intersectional *Tau-LSL-FSF-DTR* mice that carry the Cre-dependent *ROSA26-LSL-tdTomato* reporter allele. In the resulting *Tau^DTR/+;ROSA^tdTomato/+;Lbx1^Flpo/+;VT3^Cre/+* quadruple heterozygous mice, DTR expression is restricted to dorsal spinal and hindbrain neurons that coexpress VT3^Cre and Lbx1^Flpo, while all neurons with developmental VT3^Cre expression are marked with tdTomato. One month after DTX injections into adult mice, 86% of VT3^Cre-tdTomato+ neurons were eliminated in the dorsal spinal cord (Fig. 1e) and hindbrain trigeminal nuclei (Supplementary Fig. 2). No ablation was observed in other parts of the nervous system (Supplementary Fig. 2). We refer to these mice as VT3^Lbx1 neuron-ablated mice. The 14% of VT3^Cre-tdTomato+ neurons preserved in VT3^Lbx1 neuron-ablated mice (Fig. 1e, large arrowhead) potentially represent cells that lack Lbx1^Flpo expression, and the dense tdTomato+ processes in $_v$II$_i$ (Fig. 1e) likely correspond to the central terminals of the non-ablated VT3^Cre-derived DRG neurons[31].

Behavioral analyses were performed at least one month after the first DTX treatment, when transient activation of glia cells induced by cell ablation had resolved to baseline levels (data not shown). Littermates lacking DTR expression but receiving the same DTX injection served as controls. VT3^Lbx1 neuron-ablated mice showed reduced sensitivity to light von Frey filament-evoked punctate stimulations (Fig. 1f), but did not display significant changes in responses to intense noxious mechanical stimuli, such as pinpricking, pinching or intense pressure evoked by the Randall-Selitto apparatus (Fig. 1f). The ablation mice also showed normal locomotor coordination, touch and thermal sensitivity, or scratching responses evoked by various pruritogens (Supplementary Fig. 3a–i).

Impact of VT3^Lbx1 neuron ablation on mechanical hypersensitivity

We then examined two forms of mechanical hypersensitivity induced by nerve injury or inflammation: brush-evoked dynamic and filament-evoked punctate (Fig. 2a). We began by using the spared nerve injury (SNI) model to assess neuropathic mechanical hypersensitivity. VT3^Lbx1 neuron-ablated mice displayed a marked attenuation of brush-evoked dynamic hypersensitivity following SNI (Fig. 2b), in both males and females (Supplementary Fig. 4a). No significant change in filament-evoked punctate hypersensitivity (Fig. 2b) or cold allodynia (Supplementary Fig. 3j) was detected. In two inflammatory pain models induced by intraplantar injection of the complete form of Freund's adjuvant (CFA, Fig. 2c) or 3% carrageenan (Fig. 2d), we again observed a marked attenuation of dynamic, but not punctate, hypersensitivity. We next tested a lower dosage of carrageenan (0.5%), and found that the VT3^Lbx1 neuron-ablated mice could be grouped into two response clusters (Fig. 2d). The major cluster (10/16) developed robust hypersensitivity, with withdrawal thresholds (0.029 ± 0.013g) indistinguishable from those seen in control mice (0.025 ± 0.028 g; *P* = 0.71). The

minor cluster (6/16) failed to do so, and their withdrawal thresholds (0.96 ± 0.89 g) were comparable to VT3[Lbx1]neuron-ablated mice without inflammation (1.56 ± 0.80; P = 0.14) (Fig. 2d). Thus under weak inflammatory conditions, VT3[Lbx1] neurons contribute to the induction or expression of punctate hypersensitivity (see Discussion). However, these neurons are dispensable for the transmission of this form of hypersensitivity under strong inflammatory conditions or following nerve lesion.

Mechanical hypersensitivity induced by nerve injury or inflammation is caused by both neuronal sensitization and disinhibition[9–12]. To assess if the VT3[Lbx1] neurons mediate mechanical hypersensitivity induced purely by disinhibition, we performed intrathecal injection of bicuculline and strychnine to inhibit $GABA_A$ and glycine receptors, respectively. Once again, we detected a reduction in brush-evoked dynamic, but not filament-evoked punctate, mechanical hypersensitivity in VT3[Lbx1] neuron-ablated mice (Fig. 2e). In contrast, both dynamic and punctate forms of mechanical hypersensitivity induced by bicuculline and strychnine were eliminated in SOM[Lbx1] neuron-ablated mice (Supplementary Fig. 4b), consistent with reported loss of both forms of hypersensitivity induced by SNI or CFA in these ablation mice[5]. Activation of microglia following SNI, which was critical for the development of neuropathic pain[33], appears, however, unaffected in SOM[Lbx1] neuron-ablated mice (Supplementary Fig. 4c).

To further assess the requirement of VT3[Lbx1] neurons for transmission of dynamic mechanical information, we examined brush-evoked induction of c-Fos in the dorsal spinal cord. In control littermates following SNI, brushing led to induction of c-Fos in dorsal horn laminae I-V, and numbers of c-Fos^{+} neurons were greatly reduced in VT3[Lbx1] neuron-ablated mice (Fig. 3a). Brushing naïve control mice without SNI showed minimal c-Fos induction (Fig. 3a). Taken together these results indicate that VT3[Lbx1] spinal neurons transmit sensory information related to brush-evoked dynamic mechanical hypersensitivity induced by nerve injury or strong inflammation.

Silencing VT3[Lbx1] neurons attenuated pre-established dynamic mechanical hypersensitivity

To determine if VT3[Lbx1] neurons maintain a neuropathic mechanical hypersensitive state, we acutely silenced the VT3[Lbx1] neurons with the inhibitory G-protein coupled receptor hM4Di (Fig. 3b)[34,35]. To restrict hM4Di expression to spinal VT3[Lbx1] neurons, we crossed *ROSA26-LSL-FSF-hM4Di* mice with *VT3[Cre]* and *Lbx1[Flpo]* mice. The resulting triple heterozygous mice are hereafter referred to as *VT3[Lbx1]-hM4Di* (Fig. 3b). 7 and 30 days after SNI, acute silencing of VT3[Lbx1] neurons following activation of hM4Di with intrathecal injection of clozapine N-oxide (CNO)[34] attenuated brush-evoked dynamic hypersensitivity (Fig. 3c,d), without detectable change in filament-evoked punctate sensitivity (Fig. 3c,d). CNO injection in control littermates that lacked hM4Di expression did not have any effect (Fig. 3c,d). Thus, acute silencing of VT3[Lbx1] neurons reproduces phenotypes caused by VT3[Lbx1] neuron ablation (Fig. 2b). We reported previously that for NPY::Cre-marked spinal inhibitory neurons that gate mechanical itch, chemical silencing also recaptures the same phenotypes caused by neuronal ablation[35]. Thus, behavioral deficits observed in VT3[Lbx1] neuron-ablated mice are less likely due to injury responses associated with neuronal cell

ablation. More importantly, these findings indicate that VT3[Lbx1] neurons are necessary for the expression of pre-established neuropathic mechanical hypersensitivity, placing them as a valid cellular target for treating this form of pain.

Loss of brush-evoked conditional place aversion following nerve lesions in VT3[Lbx1] neuron-ablated mice

To assess the emotional/cognitive aspect of dynamic mechanical hypersensitivity, we developed a conditional place aversion (CPA) assay (Fig. 4a). The times staying in the dark chamber at pre-conditioning day 1 (t_1) and at post-conditioning day 6 (t_2) were determined, and the difference ($\Delta t = t_1 - t_2$) was used to assess the degree of CPA. We found that brushing evoked robust CPA in control littermates with SNI, with Δt reaching 339 ± 38 s compared to 19 ± 35 s in non-SNI mice (Fig. 4b,c). From this assay we conclude that the brushing from heel to toe in mice with SNI generates an unpleasant aversive feeling with mice learning to associate and avoid the "stimulation" chamber. This brush-evoked CPA following SNI was largely abolished in VT3[Lbx1] neuron-ablated mice, with Δt decreased to 56 ± 40, from 339 ± 38 in control littermates ($P < 0.001$) (Fig. 4b,c). Thus, spinal VT3[Lbx1] neurons are part of the circuits transmitting and processing the affective and/or cognitive aspects of dynamic neuropathic mechanical pain, not just mediating nocifensive motor responses.

Afferent inputs to VT3[Cre]-tdTomato^{+} neurons

In humans, brush-evoked dynamic allodynia is transmitted via myelinated Aβ (and possibly, Aδ) mechanoreceptors[14,15,19,20]. We next assessed afferent inputs to the VT3[Cre]-tdTomato^{+} neurons. Whole-cell recordings were performed following dorsal root stimulation, first at intensities (25 µA) sufficient to activate Aβ fibers, but not Aδ or C fibers (Supplementary Fig. 5a,b)[5]. Whether an Aβ input was monosynaptic or not was determined by high frequency stimulations (Supplementary Fig. 5c–e). The recordings reveal two types of tdTomato^{+} neurons (Fig. 5a), based on detectable (type 1) or non-detectable (type 2) Aβ-evoked excitatory postsynaptic currents (EPSCs) under normal recording conditions containing artificial cerebrospinal fluid (ACSF). Type 1 neurons are dominant (65%, 24/37) in the dorsal and medium lamina III ($_d$III-$_m$III), whereas type 2 cells are dominant (82%, 27/33) in the dorsal and medium part of lamina II (II$_o$-$_d$II$_i$). These two types are more mixed in the II-III border area ($_v$II$_i$-$_d$III), with types 1 and 2 representing 56% (48/86) and 41% (38/86) of VT3[Cre]-tdTomato^{+} neurons, respectively. As described in Supplementary Fig. 1c, 38% of VT3[Cre]-tdTomato^{+} neurons in $_v$II$_i$-$_d$III coexpress SOM. We reported previously that all SOM lineage neurons in this area receive Aβ-evoked EPSCs under normal conditions[5], fitting the definition of type 1 cells. Thus, a majority of type 1 VT3[Cre]-tdTomato^{+} neurons in $_v$II$_i$-$_d$III (38%/56% = 68%) must coexpress SOM. Meanwhile, by the virtue of the lack of Aβ inputs under normal conditions, type 2 cells do not belong to SOM lineage neurons. The latency of Aβ-evoked EPSCs in type 1 cells are in the range of 1.6 – 7.8 ms. At least 56% (48/86) and 79% (27/34) of type 1 cells in $_v$II$_i$-$_d$III and $_d$III-$_m$III, respectively, receive monosynaptic Aβ inputs, based on their ability to follow high frequency stimulations (20 Hz, latency variation < 0.5 ms) (Supplementary Fig. 5c–e). By holding at –45 mV to facilitate the detection of evoked inhibitory postsynaptic currents (IPSCs), we also found

that most type 1 neurons received Aβ-evoked IPSCs (Supplementary Fig. 6a–c), indicating feedforward inhibition.

We then used the current clamp to record excitatory postsynaptic potentials (EPSPs). The stimulation of Aβ fibers was unable to evoke action potential (AP) firing in 91–98% of VT3[Cre]-tdTomato^{+} neurons (Fig. 5a and Supplementary Fig. 6c). To determine if the lack of AP firing is due to feedforward inhibition, we recorded under disinhibition conditions with the presence of bicuculline and strychnine to block GABA$_A$ and glycine receptors, respectively. We found that type 1 neurons now generated Aβ-evoked AP firing (Fig. 5b and Supplementary Fig. 6d). Meanwhile, a majority of type 2 neurons started to receive a new form of Aβ-evoked EPSCs with slow onset (latencies over 10 ms) and long duration (duration over 50 ms), resulting in prolonged AP firing (Fig. 5b and Supplementary Fig. 6d). Such slow Aβ currents also emerged in most type 1 cells under disinhibition conditions (Fig. 5b and Supplementary Fig. 6d).

We next performed pharmacological studies to assess the nature of fast and slow Aβ inputs. Most primary afferents, including Aβ fibers, use glutamate for fast synaptic transmission[29]. We found that application of 10 μM of CNQX (6-cyano-7-nitroquinoxaline-2,3-dione), an antagonist for non-NMDA (N-Methyl-D-aspartic acid or N-Methyl-D-aspartate) glutamate receptors, eliminated both fast and slow Aβ inputs in randomly selected neurons from lamina III to lamina I (data not shown), indicating that transmission of Aβ inputs requires the activation of non-NMDA receptors. We then found that application of 50 μM of APV (2-Amino-5-phosphonopentanoic acid), an antagonist of NMDA receptors, failed to block fast Aβ-evoked EPSCs in type 1 cells, but did prevent them from firing APs under disinhibition conditions (Fig. 5c and Supplementary Fig. 6d). Meanwhile, APV treatment led to a complete loss of slow-onset/long-lasting Aβ inputs in both type 1 and type 2 VT3[Cre]-tdTomato^{+} neurons (Fig. 5c and Supplementary Fig. 6d), as well as in randomly picked neurons in laminae I/II$_o$ (data not shown), consistent with previous reports[36,37].

Collectively, the above recordings indicate that under normal conditions, types 1 VT3[Cre]-tdTomato^{+} neurons receive fast Aβ inputs that mainly contain non-NMDAR-mediated currents, and these inputs are insufficient to activate NMDARs and to fire APs due to feedforward inhibition (Supplementary Fig. 6e). Under disinhibition conditions, Aβ inputs now evoked both non-NMDAR and NMDAR-mediated currents that collectively drive AP firing. Type 2 cells receive Aβ inputs only under disinhibition conditions, potentially via type 1 cells (Supplementary Fig. 6e). Since NMDA receptors exhibit slow kinetics during both activation and decay phases[38], latencies of the first Aβ-evoked AP in 92% (22/24) of type 1 cells are more than 20 ms (Fig. 5b), which could explain slow-onset but long-lasting Aβ inputs in type 2 cells under disinhibition conditions (Fig. 5a,b) if they receive inputs from type 1 or type 1-like neurons (Supplementary Fig. 6e). Type 1 and type 2 cells also display distinct firing patterns following current injection, with type 1 and type 2 cells dominant with phasic and delayed firing, respectively (Fig. 5d and Supplementary Fig. 6f). Furthermore, both types of cells are divided into two subtypes based on differential responses to stimulations at intensities sufficient to activate Aδ and/or C fibers (Supplementary Fig. 7). It should be noted that type 2 cells with delayed firing were not observed in spinal cord neurons marked by the transgenic *VT3::Cre*[26].

Nerve injury-induced Aβ inputs to I/II$_o$ neurons affected by ablation of VT3^{Lbx1} or SOM^{Lbx1} neurons

We next examined how neuronal ablation affected nerve injury-induced Aβ inputs to neurons in laminae I and II$_o$, where a subset of pain output neurons is located[29]. To do this, SNI underwent at P18–21, and slice recordings were performed at P27–31. In control mice without SNI, 37% (17/46) of neurons in laminae I and II$_o$ received small fast Aβ inputs, most of which did not fire APs (Fig. 6a and Supplementary Fig. 8). Following SNI, neurons receiving Aβ inputs were increased to 80% (57/71, Chi-square test, $P < 0.001$) and of these 46% (31/68) generated AP firing, increased from 9% (4/46) in naïve mice (Chi-square test, $P < 0.001$) (Fig. 6a and Supplementary Fig. 8). Aβ-evoked EPSCs include fast-onset (latency less than 8 ms), slow-onset (latency over 10 ms) with long durations (over 50 ms), or both types (Fig. 6a and Supplementary Fig. 8). In VT3^{Lbx1} neuron-ablated mice with SNI, the percentages of I/II$_o$ neurons containing fast-onset Aβ-evoked EPSCs (59%, 42/71) or AP firing (27%, 19/71) were not different from that in control mice with SNI (59%, 42/71, Chi-square test, $P = 1.000$; 29%, 20/68, Chi-square test, $P = 0.728$). In contrast, there was a great loss of neurons with slow-onset Aβ-evoked EPSCs, from 63% (45/71) in control mice to 11% (8/71, Chi-square test, $P < 0.001$) in ablated mice (Fig. 6a,b and Supplementary Fig. 8). Furthermore, the few neurons retaining slow Aβ inputs failed to fire APs. As a result, only fast-onset Aβ-evoked AP firing induced by SNI was observed in VT3^{Lbx1} neuron-ablated mice (Fig. 6b and Supplementary Fig. 8). Consistent with the requirement of VT3^{Lbx1} neurons for the transmission of slow Aβ inputs to most superficial dorsal horn laminae, VT3^{Cre}-tdTomato$^+$ neurons generated Aβ-evoked AP firing following nerve injury (Supplementary Fig. 9). Similarly, under disinhibition conditions induced by the presence of bicuculline and strychnine, the percentage of neurons located at laminae I and II$_o$ that generated slow-onset Aβ-evoked AP firing was again selectively reduced in VT3^{Lbx1} neuron-ablated mice (Supplementary Fig. 10). In contrast, SOM^{Lbx1} neuron-ablated mice showed a loss of both fast and slow components induced by nerve injury (Fig. 6c and Supplementary Fig. 8).

The above recordings reveal two pathways linking Aβ inputs to neurons in laminae I and II$_o$ (Supplementary Fig. 11, "1", "2"). The fast pathway (Supplementary Fig. 11, "2"), which is eliminated in SOM^{Lbx1} neuron-ablated mice but preserved in VT3^{Lbx1} neuron-ablated mice, likely reflects direct (not necessarily monosynaptic) Aβ inputs onto vertical cells whose dendrites are present in lamina III. The slow polysynaptic Aβ pathway (Supplementary Fig. 11, "1") is transmitted via type 1 and/or type 2 VT3^{Cre}-tdTomato$^+$ neurons (Supplementary Fig. 11, "A"), with a majority of type 1 cells in $_v$II$_i$-III receiving monosynaptic inputs. The convergence of VT3^{Lbx1}-dependent slow inputs to a subset of vertical cells in I/II$_o$ (Supplementary Fig. 11, "B") is indicated by the observation that while the percentage of neurons that contain fast Aβ components is not changed between control and VT3^{Lbx1} neuron-ablated mice, neurons containing dual fast and slow components with AP firing were no longer detected in VT3^{Lbx1} neuron-ablated mice (Fig. 6b and Supplementary Fig. 8), indicating their conversion to fast-only neurons. As described above, many type 1 VT3^{Cre}-tdTomato$^+$ cells coexpress SOM (Fig. 1) and the vertical cells include SOM lineage neurons[5].

Morphine resistance of VT3^{Lbx1} neuron-dependent spinal pathways

Neuropathic pain patients show inconsistent responses to morphine treatment[39]. We then asked if VT3^{Lbx1} neuron-dependent and -independent spinal pathways likewise respond differentially to morphine. To test this, we first examined morphine effects on mechanical hypersensitivity induced by SNI. In control littermates, intrathecal injection of 1 nmol of morphine at day 7 after SNI inhibited filament-evoked punctate hypersensitivity (Fig. 7a). This morphine sensitivity was no longer observed at day 30 following SNI (Fig. 7a), analogous to the situation seen in rats[40]. In VT3^{Lbx1} neuron-ablated mice, both morphine-sensitive and morphine-resistant components remained intact (Fig. 7a). Dynamic hypersensitivity at either day 7 or day 30 was unaffected by intrathecal morphine injection at the dosage of 1 nmol (Fig. 7b) or 5 nmol (data not shown) in control mice, consistent with the resistance to intrathecal morphine treatment observed in other models[16,17,41,42]. In VT3^{Lbx1} neuron-ablated mice, morphine-resistant dynamic hypersensitivity was greatly attenuated at either time point (Fig. 7b).

Spinal slice recordings showed that both slow-onset and fast-onset Aβ inputs to lamina I/II$_o$ neurons induced by nerve injury were resistant to morphine (Fig. 7c,d and Supplementary Fig. 12a). We also assessed Aβ inputs opened by bicuculline and strychnine. We reported previously that only slow-onset, possibly polysynaptic Aβ inputs with AP firing are opened under this disinhibition condition[5]. These slow Aβ inputs, which are largely dependent on VT3^{Lbx1} neurons (Supplementary Fig. 10), were again resistant to morphine treatment (Fig. 7c and Supplementary Fig. 12a), at the dosage (25 μM) sufficient to suppress other spinal pathways (see below). Accordingly, removal of these slow inputs in VT3^{Lbx1} neuron-ablated mice and in SOM^{Lbx1} neuron-ablated mice likely causes the loss of morphine-resistant dynamic allodynia.

Gated C fiber inputs to $_v$II$_i$ neurons and their transmission via SOM^{Lbx1} neurons

The preservation of morphine-resistant fast Aβ inputs to I/II$_o$ neurons (Fig. 7c) might be a candidate for mediating morphine-resistant punctate hypersensitivity preserved in VT3^{Lbx1} neuron-ablated mice. To search for candidate pathways mediating morphine-sensitive punctate hypersensitivity preserved in VT3^{Lbx1} neuron-ablated mice, we next recorded C-fiber inputs to neurons located in lamina $_v$II$_i$. This region is innervated by C-LTMRs expressing the tyrosine hydroxylase and is also right adjacent to the central terminals originating from nociceptors expressing the G-protein coupled receptor MrgprD, both of which are involved in punctate mechanical hypersensitivity[23,31,43]. Characterization of C-fiber inputs to $_v$II$_i$ neurons is, however, difficult due to masking by fast and slow Aβ inputs, particularly under disinhibition conditions. To overcome this, we developed a new slice preparation that eliminated electrically low threshold Aβ inputs, by moving the second cut to a more lateral position (Fig. 7d), taking advantage of the fact that low threshold Aβ fibers enter the dorsal horn via the dorsal funiculus[31]. In this preparation, stimulations at the Aβ intensity (25 μA) failed to generate EPSCs in neurons in laminae I–III, even with the presence of bicuculline and strychnine (Fig. 7d). C intensity stimulations (500 μA, 0.1 ms) evoked detectable EPSCs in 47% (14/30) of VT3^{Cre}-negative neurons (tdTomato-negative cells in VT3^{Cre}-tdTomato mice) located in $_v$II$_i$, but these inputs failed to evoke AP firing under our recording conditions (Fig. 7d). In the presence of bicuculline and strychnine, 72%

(23/32) of these neurons fired APs (Fig. 7d and Supplementary Fig. 12b), a subset of which received a new form of electrically high threshold Aβ inputs (based on latencies < 6 ms, see Supplementary Fig. 5) without AP firing (see below, Fig. 8b). Among VT3[Cre]-negative neurons firing C-evoked APs, 68% (13/19) were inhibited by 25 μM morphine (Fig. 7d and Supplementary Fig. 12b). Bath application of 25 μM morphine caused direct hyperpolarization only in a small subset of dorsal horn neurons (Supplementary Fig. 12c), suggesting that morphine-mediated inhibition might operate mainly on primary afferents. Furthermore, following nerve lesions (SNI), 50% (5/10) of neurons in $_vII_i$ generated C-evoked AP firing (Supplementary Fig. 13), in comparison with none (0/30, Chi-square test, $P < 0.001$) in slices from naïve mice without SNI under our recording conditions (Fig. 7d; left bottom trace). Thus, VT3[Cre]-negative neurons in $_vII_i$ receive C fiber inputs with feedforward inhibition, and these gated C pathways become sensitized following nerve injury.

We next asked how C-fiber inputs to $_vII_i$ neurons are affected in VT3[Lbx1] and SOM[Lbx1] neuron-ablated mice, again using the slice preparation removing Aβ inputs (Fig. 8a) and performing recordings under the presence of bicuculline and strychnine (Fig. 8c–d). No significant change in the percentage of $_vII_i$ neurons with C-evoked AP firing was detected between control mice (64%, 23/36) and VT3[Lbx1] neuron-ablated mice (57%, 13/23; Chi-square test, $P > 0.05$) (Fig. 8b,c). However, in SOM[Lbx1] neuron-ablated mice, the percentage of neurons with C-evoked AP firing was reduced to 10% (2/20), and C-fiber inputs to the remaining 90% of $_vII_i$ neurons were either lost or reduced to the levels that were incapable of firing APs under our recording conditions (Fig. 8d). All together, we have identified three gated spinal pathways (morphine-resistant fast Aβ inputs, and morphine-sensitive/resistant C inputs) that are eliminated in SOM[Lbx1] neuron-ablated mice but preserved in VT3[Lbx1] neuron-ablated mice, and these pathways could serve as candidates for mediating morphine-sensitive and morphine-resistant punctate hypersensitivity (Supplementary Fig. 14).

Discussion

Spinal substrates transmitting acute or chronic punctate mechanical information

Our studies reveal a difference in the spinal substrates transmitting light versus intense acute punctate mechanical information. VT3[Lbx1] neurons are involved in transmitting acute light punctate mechanical information evoked by von Frey filaments but are dispensable for the transmission of superthreshold punctate stimuli evoked by pinpricking, as well as other forms of intense mechanical pain (Fig. 1). Other studies show that primary afferents expressing MrgprD, which innervate $_dII_i$, are required to sense light punctate force[23], whereas pinprick-evoked mechanical pain is mediated via thinly myelinated Aδ afferents expressing NPY2R[44]. Consistently, type 2a VT3[Cre]-marked neurons in II_o-$_dII_i$ receive inputs from C fibers but not from Aδ fibers (Supplementary Fig. 7b).

Our studies also show the dissociation in the spinal substrates transmitting acute versus chronic punctate mechanical information. Following nerve injury or inflammation, central sensitization and/or disinhibition opens the "gate". This opening allows subthreshold inputs from low threshold mechanoreceptors (A-LTMRs or C-LTMRs) to induce action potential firing in laminae I/II_o output neurons[10–12,45], causing a drastic drop in withdrawal

thresholds. The recruitment of LTMR-mediated new pain pathways could then explain why VT3^{Lbx1} neurons are largely dispensable for transmitting punctate hypersensitivity following nerve lesion or inflammation, despite being required to transmit acute light punctate mechanical stimuli. Both acute and chronic forms of punctate mechanical sensitivity are abolished in SOM^{Lbx1} neuron-ablated mice[5], suggesting chronic punctate mechanical hypersensitivity can be transmitted via a subset of SOM^{Lbx1} neurons preserved in VT3^{Lbx1} neuron-ablated mice. Our data, however, do not rule out a redundant role of VT3^{Lbx1} neurons in mediating punctate hypersensitivity (Supplementary Fig. 14).

Do distinct spinal substrates transmit dynamic versus punctate mechanical hypersensitivity?

Despite preserving punctate mechanical hypersensitivity, ablating spinal VT3^{Lbx1} neurons leads to a marked deficit in brush-evoked dynamic mechanical hypersensitivity induced by nerve lesions, inflammation, or central blockage of GABA/glycine receptors. In developing a robust conditional place aversion (CPA) assay, we further showed that spinal VT3^{Lbx1} neurons are required for transmitting the affective/cognitive aspect of dynamic neuropathic mechanical pain[46]. Electrophysiological recordings then reveal that VT3^{Cre} neurons form morphine-resistant polysynaptic pathways that relay Aβ inputs from lamina III to lamina I (Supplementary Fig. 14, pathway "1"). Our studies also reveal multiple VT3^{Lbx1} neuron-independent gated spinal pathways that become open following nerve injury, including direct Aβ inputs to vertical neurons in laminae I/II$_o$ (Supplementary Fig. 14, pathway "2") as well as C fiber inputs to VT3^{Cre}-negative neurons in $_v$II$_i$ (Supplementary Fig. 14, pathway "3"). These pathways could mediate punctate mechanical hypersensitivity preserved in VT3^{Lbx1} neuron-ablated mice. All these pathways are eliminated in SOM^{Lbx1} neuron-ablated mice (Supplementary Fig. 14), potentially explaining loss of both dynamic and punctate hypersensitivity in these mice.

Two models would account for the loss of dynamic, but the preservation of punctate, mechanical hypersensitivity in VT3^{Lbx1} neuron-ablated mice. The first model proposes the existence of spinal circuits transmitting distinct forms of mechanical hypersensitivity, with VT3^{Lbx1} neurons forming circuits involved selectively in brush (touch)-evoked dynamic allodynia. Recently a class of Aβ field-LTMRs forming circumferential endings around hair follicles was shown to respond to gentle stroking across the skin, but not to light punctate mechanical stimuli[47], making them an attractive candidate mediating dynamic allodynia. Alternatively, brushing a large skin area activate a spectrum of LTMRs, and temporal and/or spatial summation of these LTMR inputs might be required to activate VT3^{Lbx1} neuron-dependent circuits to mediate dynamic allodynia. Future *in vivo* or *ex-vivo* recordings are needed to test this possibility. The second model postulates that the VT3^{Lbx1} neuron-dependent polysynaptic circuit is one of several redundant spinal pathways that transmit mechanical allodynia, and brushing might represent a lower force stimulus compared with von Frey filament stimulation. Accordingly, the stronger von Frey filament stimulation might produce a level of VT3^{Lbx1} neuron-independent pathway activity sufficient for generating withdrawal responses in ablation mice. In contrast, the weaker brushing stimulus might require a summation of inputs from both VT3^{Lbx1} neuron-dependent and independent

pathways to drive nocifensive behaviors, leading to impaired dynamic allodynia in VT3[Lbx1] neuron-ablated mice.

The morphine experiments done at day 7 following nerve injury lend support for the first model, revealing the existence of a morphine-sensitive spinal pathway necessary for punctate, but not dynamic, hypersensitivity. The second model appears to be supported by the finding that when the concentration of carrageenan was reduced to 0.5%, only two thirds of the VT3[Lbx1] neuron-ablated mice developed punctate mechanical hypersensitivity (Fig. 2). Weak inflammation might drive suboptimal sensitization of the VT3[Lbx1] neuron-dependent and -independent pathways, making them both necessary for the full expression of punctate hypersensitivity. However, this data does not necessarily argue against the first model. VT3[Lbx1] neurons could play a minor role for the induction of punctate hypersensitivity, but once allodynia is fully induced via VT3[Lbx1] neuron-independent mechanisms, the VT3[Lbx1] neurons become dispensable for the expression of punctate allodynia.

Implication for preclinical and clinical studies

Irrespective of which model is correct, our studies show that VT3[Lbx1] neurons are necessary for the expression of brush (touch)-evoked dynamic allodynia. Furthermore, acute silencing of VT3[Lbx1] neurons attenuates pre-established dynamic neuropathic mechanical pain, indicating that these neurons are a valid cellular target for treating this form of pain. Our analyses also suggest that the von Frey filament assay lacks the resolution to reveal the selective loss of this form of pain induced by nerve lesions or strong inflammation. As such, our findings highlight a major paradox in current pre-clinical pain studies that predominantly measure von Frey filament-evoked punctate mechanical allodynia, despite the fact that touch-evoked dynamic allodynia is the major issue for neuropathic pain patients[13]. The lack of attention to the measurement of clinically more relevant dynamic allodynia could contribute to the failure in translating preclinical successes into new pain medicines[48,49]. Furthermore, the existence of multiple gated spinal pathways with differential morphine sensitivity might explain why different cohorts of patients show inconsistent responses to morphine treatment[39]. Thus, it becomes critical to develop mechanism/phenotype-based clinical trials and treatments for different cohorts of chronic pain patients[50].

METHODS

Methods, including statements of data availability and any associated accession codes and references, are available in the online version of the paper.

ONLINE METHODS

Experimental animals

All animal experiments, including behavioral tests, were performed with protocols approved by the Institutional Animal Care and Use Committee at Dana-Farber Cancer Institute, and followed NIH guidelines. Mice were housed at room temperature with a 12 h/12 h light/dark cycle and *ad libitum* access to standard mouse lab pellet food and water.

To generate *Vglut3-ires-Cre* (*VT3^Cre*) knock-in mice, a cassette containing the Cre recombinase gene preceded by an internal ribosomal entry sequence (*ires*) was targeted just distal to the stop codon of the endogenous *Vglut3 (Slc17a8)* allele so that the endogenous *Vglut3* promoter drives Cre recombinase expression. In brief, a 129 BAC genomic clone containing the *Vglut3* (also known as *Slc17a8*) gene was used to target a cassette containing the *Cre* recombinase gene preceded by an internal ribosomal entry sequence (*ires-CreFKF*)[51] just distal to the stop codon. A PCR amplicon containing the *ires-CreFKF* cassette was amplified with a forward primer containing 50 bases of *Vglut3* homology sequence including the stop codon and 20 bases of *ires-CreFKF* sequence beginning at the *ires* sequence and a reverse primer containing 50 bases of *Vlgut3* homology sequence starting 3 bases after the stop codon and 20 bases corresponding to the 3′ end of the *ires-CreFKF* cassette. The PCR amplicon was then transformed into electrocompetent EL250 bacteria containing the aforementioned *Vglut3* BAC. Homologous recombination in EL250 cells was induced as previously described[52,53] to insert the *ires-CreFKF* cassette into the *Vglut3* BAC 3 bases downstream of the stop codon. The Cre coding sequence was confirmed by DNA sequencing. The *Vglut3-ires-CreFKF* targeting construct was prepared using a commercially available kit (Qiagen, Valencia, CA), linearized, and electroporated into W4 ES cells. Targeted clones were injected into blastocysts. Chimeras were obtained and bred for germline transmission of the *Vglut3-ires-CreFKF* targeted allele. Offsprings carrying the *Vglut3-ires-CreFKF* targeted allele were subsequently bred to *Flpe* recombinase mice[54] to remove the *FKF* cassette, referred to as *VT3^Cre* mice.

The generation of mice carrying *SOM-ires-Cre* (*SOM^Cre*)[55], *ROSA26-LSL-tdTomato*[28], *Lbx1^Flpo*[5,32], *Tau-LSL-FSF-DTR*[5,32] and *ROSA26-LSL-FSL-hM4Di*[34] had been described previously.

To ablate DTR-expressing neurons for behavioral and histochemical studies, both male and female mice at 6–10 weeks old were intraperitoneally injected with diphtheria toxin (DTX, 50 μg/kg; Sigma-Aldrich, D0564) at day 1 and then again at day 4. Behavioral and histochemical experiments were performed 4 weeks after DTX injection. For characterization of VT3^Cre-tdTomato^+ neurons, spinal cords from 2–3 mice at P4, P7 and P60 were used. For quantitative histochemical studies comparing control and VT3^Lbx1 neuron-ablated mice, 3 pairs of 2–3-month old control and ablated mice were used. For each behavioral analysis, 5–17 pairs of 10–14-week old ablated and control littermates, including males and females, were used. To ablate DTR-expressing neurons for electrophysiological recording, mice (P18–P21) were intraperitoneally injected with diphtheria toxin (DTX, 50 μg/kg) at day 1 and then again at day 4. Recordings were performed 9–12 days after the first DTX injection (P27–P31). Animals were assigned in treatment groups in a blinded and randomized fashion and pain responses were measured in a blinded manner.

In Situ Hybridization (ISH) and Immunohistochemistry

In situ hybridization procedures have been described previously[56,57]. Immunohistochemistry on spinal cord sections was performed using rabbit anti-NK1R (1:1000, Sigma-Aldrich, S8305)[5], rabbit anti-PKCγ (1:400, Santa Cruz, sc-211)[5], IB4-biotin (10 μg/ml, Sigma-Aldrich, L2140)[5] and goat anti-Iba1 (1:1000, Abcam, ab5076)[32] diluted in 0.2% of Triton

X-100 plus 10% of normal goat or donkey serum in PBS. The ISH/Tomato double staining was performed as previously described[56,57]. Both fluorescent and ISH signals were collected using a fluorescent microscope. The tdTomato fluorescent signal was first photographed, followed by ISH. The pseudo fluorescent ISH signals (for VGLUT2, VGLUT3, SOM, GAD1 and GlyT2) were converted from bright field images and then merged onto the tdTomato images by the Photoshop software. Quantitative experiments were done in at least 3 animals. For each animal, at least 3 different spinal section images were taken. The software Image J (Fuji) software was used to measure the average of fluorescence intensity for evaluating the expression level of Iba1 in the whole dorsal horn prepared from mice 7 days after spared nerve injury.

Surgery, Hindpaw Injection of Inflammatory Reagents, and Intrathecal Injection of Bicuculline plus Strychnine, or Morphine

Surgery for establishing the spared nerve injury (SNI) model of neuropathic pain was performed as described previously[5,58]. For behavioral tests, adult control and ablated male and female mice (10–14 weeks) underwent surgery and animals were subjected to testing at 1–30 days after nerve injury in the lateral plantar region of the left hindpaw that was innervated by the remaining sural nerve. For whole-cell patch recordings, control and ablated mice at P18-P21 were performed with SNI surgery and animals were sacrificed for recording 9–12 days later. For CFA or carrageenan-induced inflammation, mice were briefly anesthetized with isofluorane (3–5 min at 2%), and 20 μl of Complete Freund's Adjuvant (CFA, Sigma-Aldrich, F5881) or 3% or 0.5% carrageenan (Sigma-Aldrich, C1013) was injected into the plantar surface of the left hindpaw. Behavioral testing was performed 1 day and 3 days after CFA, and 24 hours after carrageenan treatment. For allodynia induction by *in vivo* blockage of $GABA_A$ receptors and glycine receptors, 10 μl saline containing bicuculline (Sigma-Aldrich, 14340) and strychnine (Sigma-Aldrich, S0532) was injected into spinal cord intrathecally. To avoid excessive and prolonged acute "seizure-like" behaviors, including biting, vocalization and scratching responses, we first titrated the dose of bicuculline and strychnine and found that 0.02 μg bicuculline and 0.05 μg strychnine only caused short-lasting (less than 5 min) biting and scratching at the flank and low abdomen regions. We then started to measure mechanical allodynia 10 min after injection. Morphine (Patterson Veterinary Supply, 1 nmol or 5 nmol, 10 μl with saline) or saline control (10 μl) was injected intrathecally and then behavioral tests were performed following injection. Both punctate and dynamic forms of mechanical hypersensitivity were measured for 60 min after morphine injection and the peak of analgesic effect of morphine for punctate mechanical hypersensitivity was 30 min after injection. Pilot injection of 10 nmol appeared to cause motor deficits and scratching (not shown), and we did not further test this dosage.

Behavioral Testing

For all experiments, the investigator performing behavioral tests was blinded to genotypes and treatments. All data points were included for subsequent statistical analyses. All control animals were littermates of VT3[Lbx1] neuron-ablated mice, thus as a whole population, they had the same B6/129 mixed-genetic background.

The following behavioral assays have been described previously[5]: Rota-Rod, light touch, sticky tape, acetone, cold plate, hot plate, Hargreaves, von Frey, pinprick, pinch, punctate and dynamic mechanical hypersensitivity, as well as itch behavioral tests. For behavioral tests, we habituated mice for 30 min per day and for 3 consecutive days before testing. We performed most of acute behavioral tests in 4 days in the order of Rota-Rod, light touch, and sticky tape (at day 1); von Frey and Hargreaves (at day 2), hot plate and cold plate (at day 3); acetone, pinprick, pinch and Randall-selitto (at day 4). The interval was at least 2 hrs for different tests. Following acute behavioral tests, different cohorts of mice were used to test inflammatory pain, neuropathic pain (punctate and dynamic mechanical hypersensitivity were measured at the same day with at least 3 min intervals), or itch behaviors (testing 48/80 first, and then chloroquine at different days).

Tail mechanical sensitivity was measured by the Randall-Selitto device (IITC, USA). Mice were placed in a restraining plastic tube and allowed 5 min to acclimatize. Slowly increasing pressure was then applied to a point midway along the tail. The withdrawal threshold was determined by the force at which the animal showed a clear sign of discomfort or tried to escape. The test was repeated 6 times with 5 min interval.

For cold allodynia test, a drop of acetone solution was delicately dropped onto the lateral plantar surface of the paw, using a blunt needle connected to a syringe without touching the skin. The total duration of the withdrawal, flinching and licking responses was recorded.

Dynamic mechanical hypersensitivity was measured by light stroking (velocity is ~ 2 cm/s) of the external lateral side of the injured hind paw in the direction from heel to toe with a paintbrush (5/0, Princeton Art & Brush Co.). The typical response of naive mice to the dynamic mechanical stimulation is a very fast movement/lifting of the stimulated paw aside (score 0). However, after nerve injury or inflammation, several pain-suggestive responses can be observed, such as: sustained lifting (more than 2 seconds) of the stimulated paw towards the body or a single gentle flinching of the stimulated paw (score 1); one strong lateral lifting above the level of the body (what they do is like kicking to the lateral side, not like flinching, but instead more like a super hindpaw withdrawal) or a startle-like jumping (score 2), and multiple flinching responses or licking of the affected paw (score 3). Repeat the stimulation for three times at intervals of at least 3 minutes, and obtain the average score for each mouse. It should be noted that our assay is distinct from the assay used by Peirs et al., which does not distinguish baseline responses (with response rate already reaching ~60%) from dynamic mechanical hypersensitivity induced by inflammation (measured by increased rate of responses)[27]. It should also be noted that the paintbrush was prepared by trimming the tip and making it blunt. The total length of brush is about 5 mm. We then removed the outer layer of hairs. A practical suggestion is to prepare a series of paintbrushes and then test mice with or without SNI (spared nerve injury). The brush would be suitable if the average score is close to zero for naïve mice without SNI, but above 1.5 (more often around 2.0) in mice with SNI.

To measure the negative valence effect associated with brush-evoked dynamic mechanical hypersensitivity, we used a biased compartment assignment procedure, in which the influence of VT3^{Lbx1} neurons on the time of mice spending in the dark compartment

receiving conditional stimulations was measured. The conditional place aversion (CPA) apparatus consisted of two chambers ($10 \times 10 \times 15$ cm per compartment), dark ("A") and bright ("B"), and the chambers were placed onto the metal mesh (served as the chamber floor). The center was an inserted black (face to compartment "A")/white (face to compartment "B") plastic wall with a rectangular hole in the lower middle (4×8 cm) (Fig. 4a). Mouse movement was recorded by a Sony camcorder. The time a mouse spent in chamber A was evaluated by the experimenter after recording. On Day 1, each mouse was placed in the bright compartment ("B") and allowed to freely explore between chambers A and B for 15 min (pre-test). With this apparatus design, most, if not all, naïve mice showed an initial preference for dark chamber A. A four-day period of conditioning was performed. On Days 2 and 4, the hole in the central wall was blocked by covering a dark film from the dark compartment. Mouse was put in the bright chamber B for 20 min. On Days 3 and 5, the hole in the central wall was blocked by covering a dark film from the bright compartment. Mouse was then put in the dark chamber A, and the hindpaw of injured site was brushed by 5/0 paintbrusher for 20 min with ~2 sec intervals, in the direction from heel to toe. On Day 6, the dark film that covered the hole in the central wall was removed. The individual mice were tested for their side compartment preference by placing them in the bright compartment first and allowing them to freely explore the entire apparatus for 15 min (post-test). The aversion score was measured as the time (s) spent in the dark compartment during pre-test subtracted with the time (s) spent in the dark compartment during post-test.

Acute Silencing

For the silencing experiments, $VT3^{Cre/+};Lbx1^{Flpo/+};ROSA26-ds-hM4Di$ ($VT3^{Cre}-hM4Di$) mice and their control littermates were used. Mice, before or after nerve injury, were acclimatized in a chamber placed on a mesh (used as the chamber floor) for 30 min per day for 2 days before experiment. On the day of the experiment, mice were acclimated for 30 min and then briefly removed from the chamber for intraperitoneal injection of clozapine-N-oxide (CNO, Sigma-Aldrich, C0832, 5 mg/kg). Mice were then returned to the chamber. Brushed evoked dynamic mechanical hypersensitivity and filament-evoked punctate mechanical hypersensitivity were evaluated at 10 min intervals after CNO injection for 90 min. At every time point, the external lateral side of the injured hindpaw received punctate mechanical stimuli by von Frey filaments, and the thresholds causing withdrawal responses were measured using the Dixon's up-down method[16]. Then, at 3 min intervals, a 5/0 paintbrush with trimmed tip was used to stroke the external lateral side of the injured hind paw from heel to toe for 3 times at ~10 sec intervals. The average score of responses was evaluated as the dynamic score. To measure cold allodynia after silencing VT3^{Lbx1} neurons, control and $VT3^{Lbx1}-hM4Di$ mice got intraperitoneal injection of CNO 7 day after SNI. Cold allodynia (see above) that induced by acetone drop was measured 40 min after CNO injection.

C-Fos induction

To induce c-Fos expression by dynamic brush stimulations in VT3^{Lbx1} ablated and control mice, each mouse was put in a bright chamber ($10 \times 10 \times 15$ cm) with the metal mesh as the floor. A 5/0 paintbrush with trimmed tip was used to stroke the external lateral side of the injured hindpaw from heel to toe for ~600 times in a 20-min period (~2 sec intervals). Two

hours later, the lumbar spinal cord was dissected, fixed, embedded and was then sectioned as sagittal slices for further c-Fos immunostaining (rabbit anti c-Fos antibody, 1:500, Millipore, ABE457)[5].

Spinal Cord Slice Preparation

Preparation of spinal cord slice with full length of dorsal root and DRG attached had been described previously[5]. Briefly, mice (P24-P31) were deeply anesthetized with isoflurane, decapitated and the lumbar spinal cord was quickly removed to ice-cold modified artificial cerebrospinal fluid (ACSF), which contains (in mM): NaCl, 80; KCl, 2.5; NaH_2PO4, 1.25; $CaCl_2$, 0.5; $MgCl_2$, 3.5; $NaHCO_3$, 25; sucrose, 75; sodium ascorbate, 1.3; sodium pyruvate, 3.0 with pH at 7.4 and osmolality at 310–320 mOsm. The spinal cord with full length of dorsal roots and DRG attached was cut by a vibratome VT1000S (Leica, Germany), as illustrated in Fig. 7c. To eliminate low threshold Aβ-fiber inputs to dorsal horn neurons in some experiments, the slice was prepared in a way as illustrated in Fig. 7d. The slice was incubated for about 1 h at 35°C in a solution that contains (in mM): NaCl, 125; KCl, 2.5; $CaCl_2$, 2; $MgCl_2$, 1, NaH_2PO4, 1.25; $NaHCO_3$, 26; D-glucose, 25; sodium ascorbate, 1.3; sodium pyruvate, 3.0 with pH at 7.2 and measured osmolality at 310–320 mOsm, and oxygenated with 95% O_2 and 5% CO_2. The slice was then transferred into a recording chamber and perfused with oxygenated recording solution at a rate of 5 ml/min prior to electrophysiological recordings at room temperature.

Patch Clamp Recordings and Dorsal Root Stimulations

Whole cell recording experiments had been described previously[5]. Internal solution contains (in mM): potassium gluconate 130, KCl 5, Na_2ATP 4, NaGTP 0.5, HEPES 20, EGTA 0.5, pH 7.28 with KOH, and measured osmolality at 310–320 mOsm. Data were acquired with pClamp 10.0 software (Molecular Devices, USA) using MultiClamp 700B patch-clamp amplifier and Digidata 1440A (Molecular Devices, USA). Responses were low-pass filtered on-line at 2 kHz, digitized at 5 kHz.

The stimulus threshold ranges for Aβ, Aδ and C fibers are 12–16 μA, 30–35 μA and 100–300 μA, respectively, as determined previously[5]. Accordingly, the intensity ranges used in this study for different fibers are: 25 μA for Aβ, 30–50 μA for Aδ, and 100–500 μA for C fibers. We therefore used 25 μA, 50 μA and 500 μA to screen for Aβ, Aδ and C-fiber-mediated synaptic inputs/outputs in the spinal dorsal horn (pulse width 0.1 ms or 0.5 ms).

As described before[5], three types of recording conditions were performed to test primary afferent inputs to dorsal horn neurons. Firstly, by holding membrane potential at −70 mV (sometimes −80 to −85 mV), evoked inhibitory postsynaptic current (eIPSC) was minimized, so that evoked excitatory postsynaptic current (eEPSC) may be detected even if it is small. This recording condition was used to study whether a neuron receives inputs directly (mono-eEPSC) or indirectly (poly-eEPSC) from Aβ, Aδ or C fibers. Please see Supplementary Fig. 5 for the parameters to identify synaptic inputs from Aβ, Aδ and C fibers. In our recording condition, the distance from the tip of the suction electrode (stimulation electrode) to the entrance of the attached dorsal root is ~ 8 mm. Under disinhibition or nerve injury conditions, dorsal root stimulations at the low threshold Aβ

intensity range induced two types of inputs in dorsal horn neurons: 1) fast-onset inputs (latency usually less than 10 ms) and 2) slow-onset inputs, with latency usually more than 10 ms and duration usually over 50 ms (some potentially electrically low-threshold C fiber inputs, with latency more than 10 ms but duration less than 50 ms, were also included, but were excluded in our previous study[5], explaining a difference in the percentages of $_v$II$_i$-$_d$III neurons receiving slow-onset inputs under normal conditions between these two studies). Fast-onset Aβ inputs include both mono- and poly-synaptic inputs. Secondly, by holding membrane potential at −45 mV, both eEPSC and eIPSC can be detected simultaneously. Thirdly, current clamp mode at the resting membrane potential (or slightly hyperpolarized to block the generation of spontaneous AP firings) was used to record dorsal root stimulation-evoked action potentials (Aβ, Aδ and C-evoked APs), either under the normal recording solution or under dis-inhibition conditions with the presence of both bicuculline (10 μM) and strychnine (2 μM). AP firing patterns following current injections were determined from the holding membrane potentials around −85 mV.

The series resistance for all the neurons recorded in this study is within 30 mΩ, and the liquid junction potential is about 15 mV. When we randomly pick neurons, neurons in a given lamina (from control or ablated mice) were picked under the bright field microscope, without considering their sizes and morphologies. All recordings were performed at room temperature. Drugs were bath applied by exchanging perfusion solution containing a known drug concentration without altering the perfusion rate.

Statistical Analyses

Results are expressed as mean ± SEM. Statistical analyses were done using the GraphPad Prism. For locomotion coordination, touch, itch and acute pain assessment, data were subjected to the Student's *t* test. For CFA-induced inflammatory pain, SNI-induced neuropathic pain, and pain induced by intrathecal injection of bicuculline and strychnine, time-course measurements were assessed by Bonferroni's post hoc analyses of variance between groups (ANOVA). For statistical analysis of incidence of electrophysiological results, data were subjected to Chi-square test (see Supplementary Methods Checklist). All data sets were tested for normality using SigmaStat 3.5 software, if the criteria of normality and equal variance were not met, we used Mann-Whitney *U*-Test, and results were expressed as median ± quartile. The $P < 0.05$ was accepted as statistically different. No statistical methods were used to pre-determine sample sizes but our sample sizes are similar to those reported in previous publications[4,5].

Data availability

The data that support the findings of this study are available from the corresponding author upon reasonable request.

Supplementary Material

Refer to Web version on PubMed Central for supplementary material.

Acknowledgments

References

1. Melzack R, Wall PD. Pain mechanisms: a new theory. Science. 1965; 150:971–979. [PubMed: 5320816]

2. Mendell LM. Constructing and deconstructing the gate theory of pain. Pain. 2014; 155:210–216. [PubMed: 24334188]

3. Braz J, Solorzano C, Wang X, Basbaum AI. Transmitting pain and itch messages: a contemporary view of the spinal cord circuits that generate gate control. Neuron. 2014; 82:522–536. [PubMed: 24811377]

4. Lu Y, et al. A feed-forward spinal cord glycinergic neural circuit gates mechanical allodynia. J Clin Invest. 2013; 123:4050–4062. [PubMed: 23979158]

5. Duan B, et al. Identification of spinal circuits transmitting and gating mechanical pain. Cell. 2014; 159:1417–1432. [PubMed: 25467445]

6. Foster E, et al. Targeted ablation, silencing, and activation establish glycinergic dorsal horn neurons as key components of a spinal gate for pain and itch. Neuron. 2015; 85:1289–1304. [PubMed: 25789756]

7. Petitjean H, et al. Dorsal Horn Parvalbumin Neurons Are Gate-Keepers of Touch-Evoked Pain after Nerve Injury. Cell Rep. 2015 pii: S2211-1247(15)01134-1.

8. Cui L, et al. Identification of Early RET plus Deep Dorsal Spinal Cord Interneurons in Gating Pain. Neuron. 2016; 91:1137–1153. [PubMed: 27545714]

9. Price TJ, Cervero F, Gold MS, Hammond DL, Prescott SA. Chloride regulation in the pain pathway. Brain Res Rev. 2009; 60:149–170. [PubMed: 19167425]

10. von Hehn CA, Baron R, Woolf CJ. Deconstructing the neuropathic pain phenotype to reveal neural mechanisms. Neuron. 2012; 73:638–652. [PubMed: 22365541]

11. Kuner R. Spinal excitatory mechanisms of pathological pain. Pain. 2015; 156(Suppl 1):S11–17. [PubMed: 25789427]

12. Treede RD. Gain control mechanisms in the nociceptive system. Pain. 2016; 157:1199–1204. [PubMed: 26817644]

13. Truini A, Garcia-Larrea L, Cruccu G. Reappraising neuropathic pain in humans–how symptoms help disclose mechanisms. Nat Rev Neurol. 2013; 9:572–582. [PubMed: 24018479]

14. Koltzenburg M, Lundberg LE, Torebjörk HE. Dynamic and static components of mechanical hyperalgesia in human hairy skin. Pain. 1992; 51:207–219. [PubMed: 1484717]

15. Ochoa JL, Yarnitsky D. Mechanical hyperalgesias in neuropathic pain patients: dynamic and static subtypes. Ann Neurol. 1993; 33:465–472. [PubMed: 8388678]

16. Miraucourt LS, Moisset X, Dallel R, Voisin DL. Glycine inhibitory dysfunction induces a selectively dynamic, morphine-resistant, and neurokinin 1 receptor- independent mechanical allodynia. J Neurosci. 2009; 29:2519–2527. [PubMed: 19244526]

17. Field MJ, Bramwell S, Hughes J, Singh L. Detection of static and dynamic components of mechanical allodynia in rat models of neuropathic pain: are they signalled by distinct primary sensory neurones? Pain. 1999; 83:303–311. [PubMed: 10534603]

18. Samuelsson M, Leffler AS, Hansson P. Dynamic mechanical allodynia: on the relationship between temporo-spatial stimulus parameters and evoked pain in patients with peripheral neuropathy. Pain. 2005; 115:264–272. [PubMed: 15911153]

19. Torebjörk HE, Lundberg LE, LaMotte RH. Central changes in processing of mechanoreceptive input in capsaicin-induced secondary hyperalgesia in humans. J Physiol. 1992; 448:765–780. [PubMed: 1593489]

20. Campbell JN, Raja SN, Meyer RA, Mackinnon SE. Myelinated afferents signal the hyperalgesia associated with nerve injury. Pain. 1988; 32:89–94. [PubMed: 3340426]

21. Lindblom U, Verrillo RT. Sensory functions in chronic neuralgia. J Neurol Neurosurg Psychiatry. 1979; 42:422–435. [PubMed: 448382]

22. Price DD, Bennett GJ, Rafii A. Psychophysical observations on patients with neuropathic pain relieved by a sympathetic block. Pain. 1989; 36:273–288. [PubMed: 2710557]

23. Cavanaugh DJ, et al. Distinct subsets of unmyelinated primary sensory fibers mediate behavioral responses to noxious thermal and mechanical stimuli. Proc Natl Acad Sci U S A. 2009; 106:9075–9080. [PubMed: 19451647]

24. Boada MD, et al. Fast-conducting mechanoreceptors contribute to withdrawal behavior in normal and nerve injured rats. Pain. 2014; 155:2646–2655. [PubMed: 25267211]

25. Xu ZZ, et al. Inhibition of mechanical allodynia in neuropathic pain by TLR5-mediated A-fiber blockade. Nat Med. 2015; 21:1326–1231. [PubMed: 26479925]

26. Malmberg AB, Chen C, Tonegawa S, Basbaum AI. Preserved acute pain and reduced neuropathic pain in mice lacking PKCgamma. Science. 1997; 278:279–283. [PubMed: 9323205]

27. Peirs C, et al. Dorsal Horn Circuits for Persistent Mechanical Pain. Neuron. 2015; 87:797–812. [PubMed: 26291162]

28. Madisen L, et al. A robust and high-throughput Cre reporting and characterization system for the whole mouse brain. Nat Neurosci. 2010; 13:133–140. [PubMed: 20023653]

29. Todd AJ. Neuronal circuitry for pain processing in the dorsal horn. Nat Rev Neurosci. 2010; 11:823–836. [PubMed: 21068766]

30. Light AR, Trevino DL, Perl ER. Morphological features of functionally defined neurons in the marginal zone and substantia gelatinosa of the spinal dorsal horn. J Comp Neurol. 1979; 186:151–171. [PubMed: 447881]

31. Abraira VE, Ginty DD. The sensory neurons of touch. Neuron. 2013; 79:618–639. [PubMed: 23972592]

32. Bourane S, et al. Identification of a spinal circuit for light touch and fine motor control. Cell. 2015; 160:503–515. [PubMed: 25635458]

33. Ji RR, Berta T, Nedergaard M. Glia and pain: is chronic pain a gliopathy? Pain. 2013; (Suppl 1):S10–28. [PubMed: 23792284]

34. Ray RS, et al. Impaired respiratory and body temperature control upon acute serotonergic neuron inhibition. Science. 2011; 333:637–642. [PubMed: 21798952]

35. Bourane S, et al. Gate control of mechanical itch by a subpopulation of spinal cord interneurons. Science. 2015; 350:550–554. [PubMed: 26516282]

36. Baba H, et al. Removal of GABAergic inhibition facilitates polysynaptic A fiber-mediated excitatory transmission to the superficial spinal dorsal horn. Mol Cell Neurosci. 2003; 24:818–30. [PubMed: 14664828]

37. Torsney C, MacDermott AB. Disinhibition opens the gate to pathological pain signaling in superficial neurokinin 1 receptor-expressing neurons in rat spinal cord. J Neurosci. 2006; 26:1833–1843. [PubMed: 16467532]

38. Edmond B, Gibb AJ, Colquhoun D. Mechanisms of activation of glutamate receptors and the time course of excitatory synaptic currents. Annu Rev Physiol. 1995; 57:495–519. [PubMed: 7778875]

39. McNicol ED, Midbari A, Eisenberg E. Opioids for neuropathic pain. Cochrane Database Syst Rev. 2013; 8:CD006146.

40. Due MR, et al. Carbamazepine potentiates the effectiveness of morphine in a rodent model of neuropathic pain. PLoS One. 2014; 9:e107399. [PubMed: 25221944]

41. Yaksh TL. Behavioral and autonomic correlates of the tactile evoked allodynia produced by spinal glycine inhibition: effects of modulatory receptor systems and excitatory amino acid antagonists. Pain. 1989; 37:111–123. [PubMed: 2542867]

42. Sherman SE, Loomis CW. Morphine insensitive allodynia is produced by intrathecal strychnine in the lightly anesthetized rat. Pain. 1994; 56:17–29. [PubMed: 8159438]

43. François A, et al. The Low-Threshold Calcium Channel Cav3.2 Determines Low-Threshold Mechanoreceptor Function. Cell Rep. 2015 S2211-1247(14)01095-X.

44. Arcourt A, et al. Touch Receptor-Derived Sensory Information Alleviates Acute Pain Signaling and Fine-Tunes Nociceptive Reflex Coordination. Neuron. 2017; 93:179–193. [PubMed: 27989460]

45. Prescott SA, Sejnowski TJ, De Koninck Y. Reduction of anion reversal potential subverts the inhibitory control of firing rate in spinal lamina I neurons: towards a biophysical basis for neuropathic pain. Molecular Pain. 2006; 2:20. [PubMed: 16764720]

46. Bushnell MC, Ceko M, Low LA. Cognitive and emotional control of pain and its disruption in chronic pain. Nat Rev Neurosci. 2013; 14:502–511. [PubMed: 23719569]

47. Bai L, et al. Genetic Identification of an Expansive Mechanoreceptor Sensitive to Skin Stroking. Cell. 2015; 163:1783–1795. [PubMed: 26687362]

48. Cobos EJ, Portillo-Salido E. "Bedside-to-Bench" Behavioral Outcomes in Animal Models of Pain: Beyond the Evaluation of Reflexes. Curr Neuropharmacol. 2013; 11:560–591. [PubMed: 24396334]

49. Mogil JS. Animal models of pain: progress and challenges. Nat Rev Neurosci. 2009; 10:283–294. [PubMed: 19259101]

50. Reimer M, Helfert SM, Baron R. Phenotyping neuropathic pain patients: implications for individual therapy and clinical trials. Curr Opin Support Palliat Care. 2014; 8:124–129. [PubMed: 24670811]

51. Michael SK, Brennan J, Robertson EJ. Efficient gene-specific expression of cre recombinase in the mouse embryo by targeted insertion of a novel IRES-Cre cassette into endogenous loci. Mech Dev. 1999; 85:35–47. [PubMed: 10415345]

52. Lee EC, et al. A highly efficient Escherichia coli-based chromosome engineering system adapted for recombinogenic targeting and subcloning of BAC DNA. Genomics. 2001; 73:56–65. [PubMed: 11352566]

53. Liu P, Jenkins NA, Copeland NG. A highly efficient recombineering-based method for generating conditional knockout mutations. Genome Res. 2003; 13:476–484. [PubMed: 12618378]

54. Rodriguez CI, et al. High-efficiency deleter mice show that FLPe is an alternative to Cre-loxP. Nat Genet. 2000; 25:139–140. [PubMed: 10835623]

55. Taniguchi H, et al. A resource of Cre driver lines for genetic targeting of GABAergic neurons in cerebral cortex. Neuron. 2011; 71:995–1013. [PubMed: 21943598]

56. Liu Y, et al. VGLUT2-dependent glutamate release from peripheral nociceptors is required to sense pain and suppress itch. Neuron. 2010; 68:543–556. [PubMed: 21040853]

57. Lou S, Duan B, Vong L, Lowell BB, Ma Q. Runx1 controls terminal morphology and mechanosensitivity of VGLUT3-expressing C-mechanoreceptors. J Neurosci. 2013; 33:870–882. [PubMed: 23325226]

58. Decosterd I, Woolf CJ. Spared nerve injury: an animal model of persistent peripheral neuropathic pain. Pain. 2000; 87:149–158. [PubMed: 10924808]
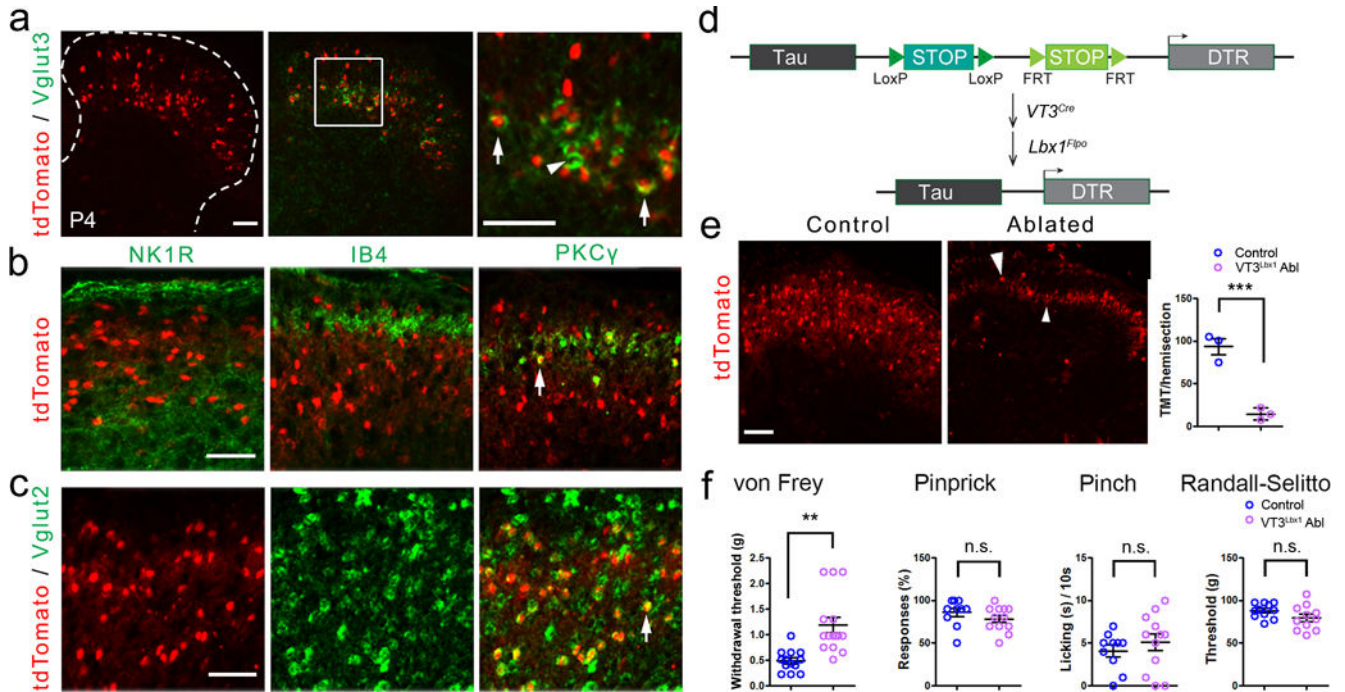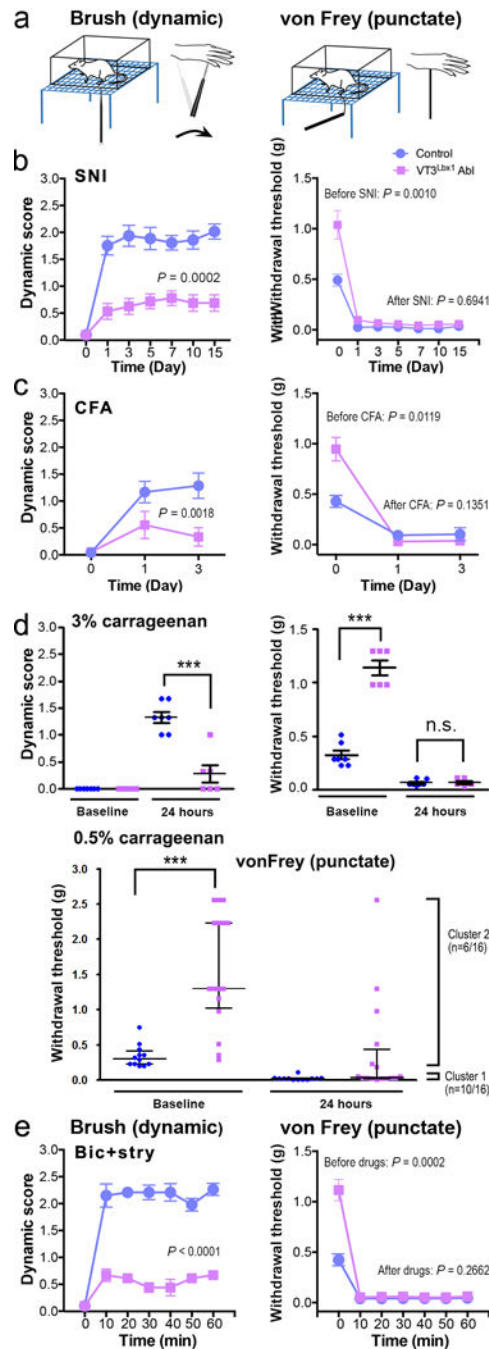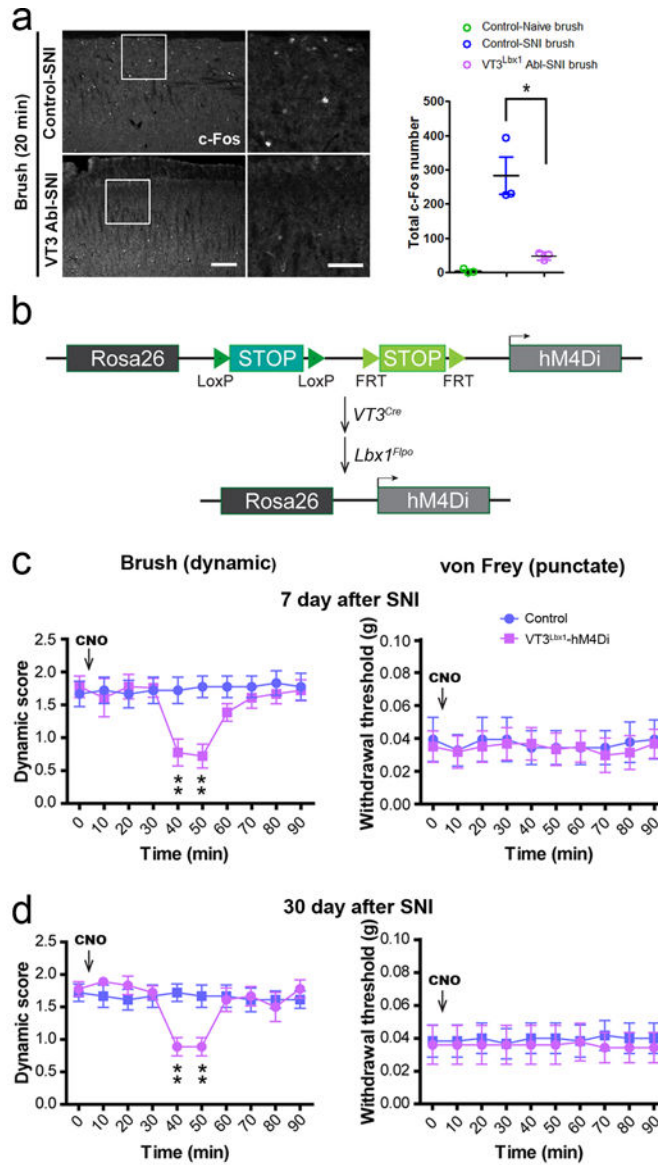
Figure 1.
Characterization of VT3^{Cre}-tdTomato neurons and punctate sensitivity in VT3^{Lbx1} neuron-ablated mice. (**a-c**) Spinal sections from P4 mice (**a**) and adult mice (**b,c**) showing tdTomato signals (red) and VGLUT3 mRNA, NK1R protein, IB4 isolectin binding, PKCγ protein, or VGLUT2 mRNA (green). Right panels in **a** represent higher magnification of the boxed areas. Arrows indicate co-localization, and arrowhead in **a** indicates a cell expressing VGLUT3 mRNA but having not yet activated tdTomato. (**d**) The intersectional genetic strategy for driving DTR expression in spinal VT3^{Lbx1} neurons. (**e**) Ablation of 86% of VT3^{Cre}-tdTomato$^+$ neurons in adult lumbar cord (Control: 96 ± 11 per hemisection, Ablated ("VT3^{Cre}-Abl") mice:14 ± 4; n = 3 mice per group; two-tailed student's unpaired t test; t_4 = 6.885, ***, P = 0.002). Large arrowhead indicates remained cells, and small arrowhead indicates processes likely from VT3^{Cre}-tdTomato$^+$ primary afferents. (**f**) Increased withdrawal thresholds to von Frey filament stimulations (n = 17, Control; n = 15, Ablated; two-tailed student's unpaired t test; t_{30} = 4.4107, **, P < 0.01). No detectable changes in pinprick responses (n = 10, Control; n = 12, Ablated; unpaired t test, t_{20} = 1.180, P = 0.2519), pinch (n = 10, Control; n = 12, Ablated; two-tailed student's unpaired t test, t_{20} = 0.7881, P = 0.4399), or Randall-Sellito (n = 11 in each group; two-tailed student's unpaired t test, t_{20} = 1.618, P = 0.1213). Scale bars are 50 μm in all images. Data are represented as mean ± SEM.

Figure 2.

Loss of dynamic mechanical hypersensitivity in VT3[Lbx1] neuron-ablated ("VT3[Lbx1] Abl") mice. (**a**) Schematics for dynamic and punctate stimulations. (**b-e**) Loss of brush-evoked dynamic hypersensitivity in VT3[Lbx1] Abl mice following SNI (**b**, left, n = 13, Control; n = 11, VT3[Lbx1] Abl; two-way ANOVA, $F_{6, 154} = 4.783$, $P = 0.0002$), CFA (**c**, left, n = 5, control; n = 6, VT3[Lbx1] Abl; two-way ANOVA, $F_{1, 24} = 12.37$, $P = 0.0018$), 3% carrageenan (**d**, top left, n = 7, control; n = 6, VT3[Lbx1] Abl; two-tailed student's unpaired t test, $t_{11} = 5.730$, $P = 0.0001$), or following Intrathecal injection of bicuculline and strychnine ("Bic

+Stry") (**e**, left, n = 6, Control; n = 6, VT3^{Lbx1} Abl; two-way ANOVA, $F_{6, 70}$ = 14.0925, $P <$ 0.0001). No changes in punctate hypersensitivity after SNI (**b**, right, n = 13, Control; n = 11, VT3^{Lbx1} Abl; before SNI, two-tailed student's unpaired t test, t_{22} = 3.798, $P =$ 0.0010; after SNI, two-way ANOVA, $F_{5, 132}$ = 0.6077, $P =$ 0.6941), CFA (**c**, right, n = 5, Control; n = 6, VT3^{Lbx1} Abl; before CFA, two-tailed student's unpaired t test, t_9 = 2.922, $P =$ 0.0119; after CFA, two-way ANOVA, $F_{1, 24}$ = 2.391, $P =$ 0.1351), 3% carrageenan assay (**d**, top right, n = 7, Control; n = 6, VT3^{Lbx1} Abl; before carrageenan, two-tailed unpaired t test; before carrageenan, t_{11} = 10.28, $P <$ 0.0001; after carrageenan, two-tailed unpaired t test, t_{11} = 0.2360, $P =$ 0.8178), or following Bic+Stry (**e**, right, n = 6, Control; n = 6, VT3^{Lbx1} Abl; before Bic+Stry, two-tailed student's unpaired t test, t_{10} = 5.811, $P =$ 0.0002; after Bic+Stry, two-way ANOVA, $F_{1, 60}$ = 1.260, $P =$ 0.2662). (**d**, bottom) 0.5% carrageenan treatment. An increase in withdrawal thresholds before inflammation (n =12, control; n =16, VT3^{Lbx1} Abl; two-tailed student's unpaired t test, t_{26} = −5.174, $P <$ 0.0001). VT3^{Lbx1} neuron-ablated mice can be divided into two clusters after inflammation. Cluster 1 (10/16) showed withdrawal thresholds (0.029 ± 0.013g; n = 10) indistinguishable from control mice (0.025 ± 0.028 g; n =12; two-tailed student's unpaired t test, t_{20} = −0.377, $P =$ 0.7100). Cluster 2 (6/16), however, showed withdrawal thresholds (0.96 ± 0.89 g; n =6) comparable to that seen in ablation mice without inflammation (1.6 ± 0.80; n =16; two-tailed student's unpaired t test, t_{20} = 1.531, $P =$ 0.1414), and significantly higher than that in control mice (0.025 ± 0.028 g; n =12; two-tailed student's unpaired t test, t_{16} = −3.74, $P =$ 0.0018). Data are represented as mean ± SEM. ***, $P <$ 0.001.

Figure 3.
Reduction of brush-evoked c-Fos in VT3^{Lbx1} neuron-ablated ("VT3^{Lbx1}-Abl") mice and attenuation of dynamic mechanical hypersensitivity by silencing VT3^{Lbx1} neurons. (**a**) c-Fos induction after brushing the hindpaw of control mice (with or without SNI) or VT3^{Lbx1}-Abl mice (with SNI) (n = 3 mice per group; two-tailed student's unpaired t test; t_4 = 4.260, *, P = 0.0131). Scale bars are 100 μm in the left images and 50 μm in the right. (**b**) Schematics showing the intersectional genetic strategy to drive hM4Di in VT3^{Lbx1} neurons. (**c,d**) Impact of VT3^{Lbx1} neuron silencing via CNO-mediated activation of hM4Di on mechanical hypersensitivity (n = 6, Control; n = 6, VT3^{Lbx1}-hM4Di). Left columns: attenuation of dynamic hypersensitivity at day 7 post SNI (**c** left, two-tailed student's unpaired t test, 40min post-CNO, t_{10} = 3.3, P = 0.0080; 50min post-CNO, t_{10} = 3.789, P = 0.0035) or at day 30 post SNI (**d**, two-tailed student's unpaired t test, 40min post-CNO, t_{10} = 4.287, P = 0.0016; 50min post-CNO, t_{10} = 3.501, P = 0.0057). Right columns: no detectable change in

punctate hypersensitivity at day 7 post SNI (two-tailed student's unpaired t test, 40min post-CNO, $t_{10} = 0.1638$, $P = 0.8732$; 50min post-CNO, $t_{10} = 0.0702$, $P = 0.9454$) and at day 30 post SNI (two-tailed student's unpaired t test, 40min post-CNO, $t_{10} = 0.2666$, $P = 0.7952$; 50min post-CNO, $t_{10} = 0.2666$, $P = 0.7952$). Data are represented as mean ± SEM. *, $P < 0.05$, **, $P < 0.01$.
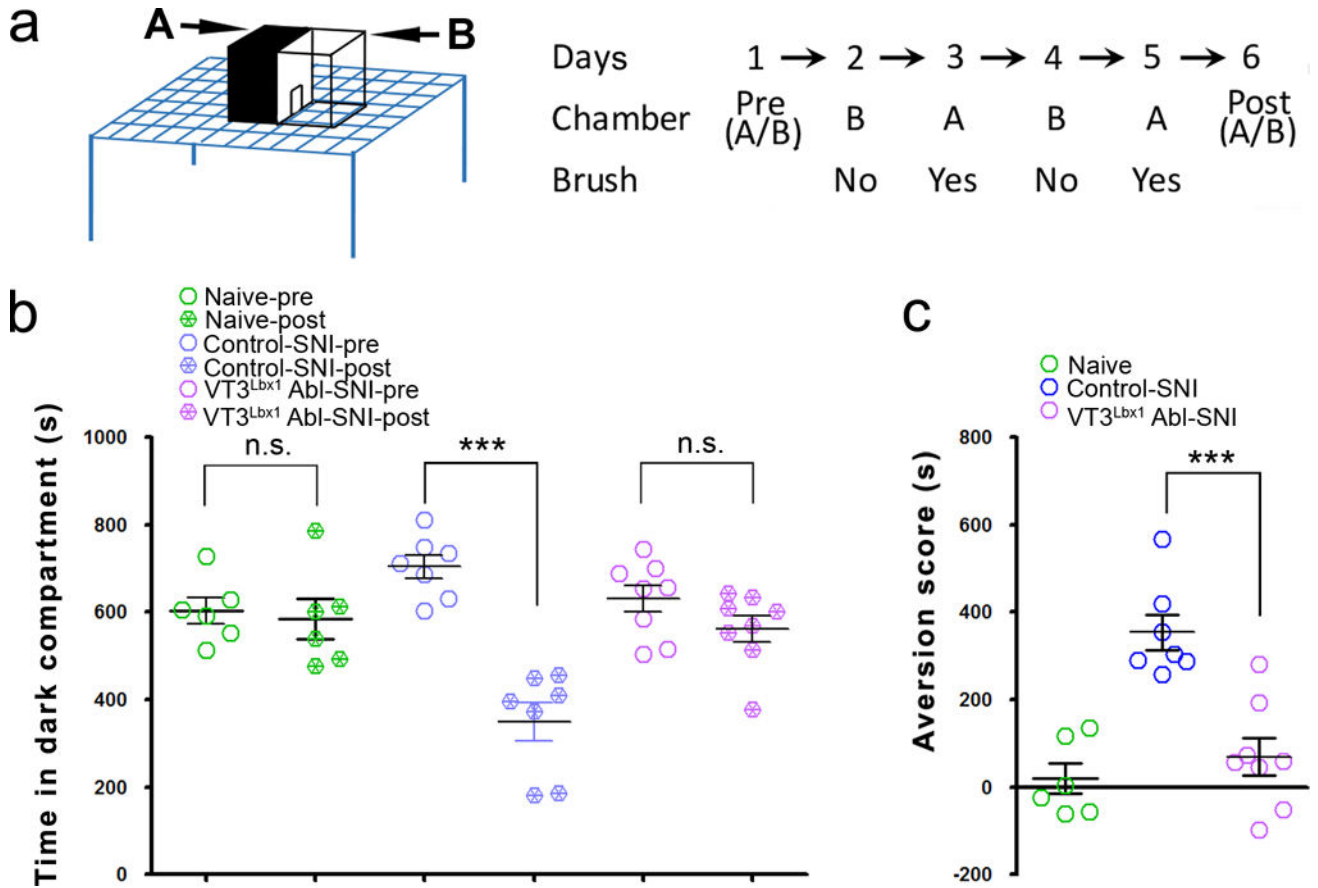
Figure 4.
Ablation of VT3^{Lbx1} neurons suppressed brush-evoked conditioned place aversion (CPA) in mice with nerve injury (SNI). (**a**) Schematics of the CPA apparatus and the experimental design. The dark and bright chambers are labeled as "A" and "B", respectively. At day 1 and day 6, the residence times in the dark A chamber during a 15-min period were determined. On days 2–5, the mouse was placed in the indicated chamber for 20 min, with or without brushing. (**b,c**) Absolute time (s) in the dark A chamber before ("pre") versus after ("post") conditioning for various experimental groups (**b**), or CPA scores defined by the time difference staying in the A chamber: (time before training) – (time after training) (**c**). n = 6, control littermates without SNI ("naïve"); n = 8, control littermates with SNI; n = 9, VT3^{Lbx1} Abl with SNI. For (**b**), two-tailed student's paired t test; naive: $t_{10} = 0.3487$, $P = 0.7345$; control-SNI: $t_{14} = 7.249$, $P < 0.0001$; VT3^{Lbx1} ablated-SNI: $t_{16} = 1.410$, $_p = 0.1777$; for (**c**), two-tailed student's unpaired t test; $t_{15} = 5.066$, ***, $P = 0.0001$. Data are represented as mean ± SEM.
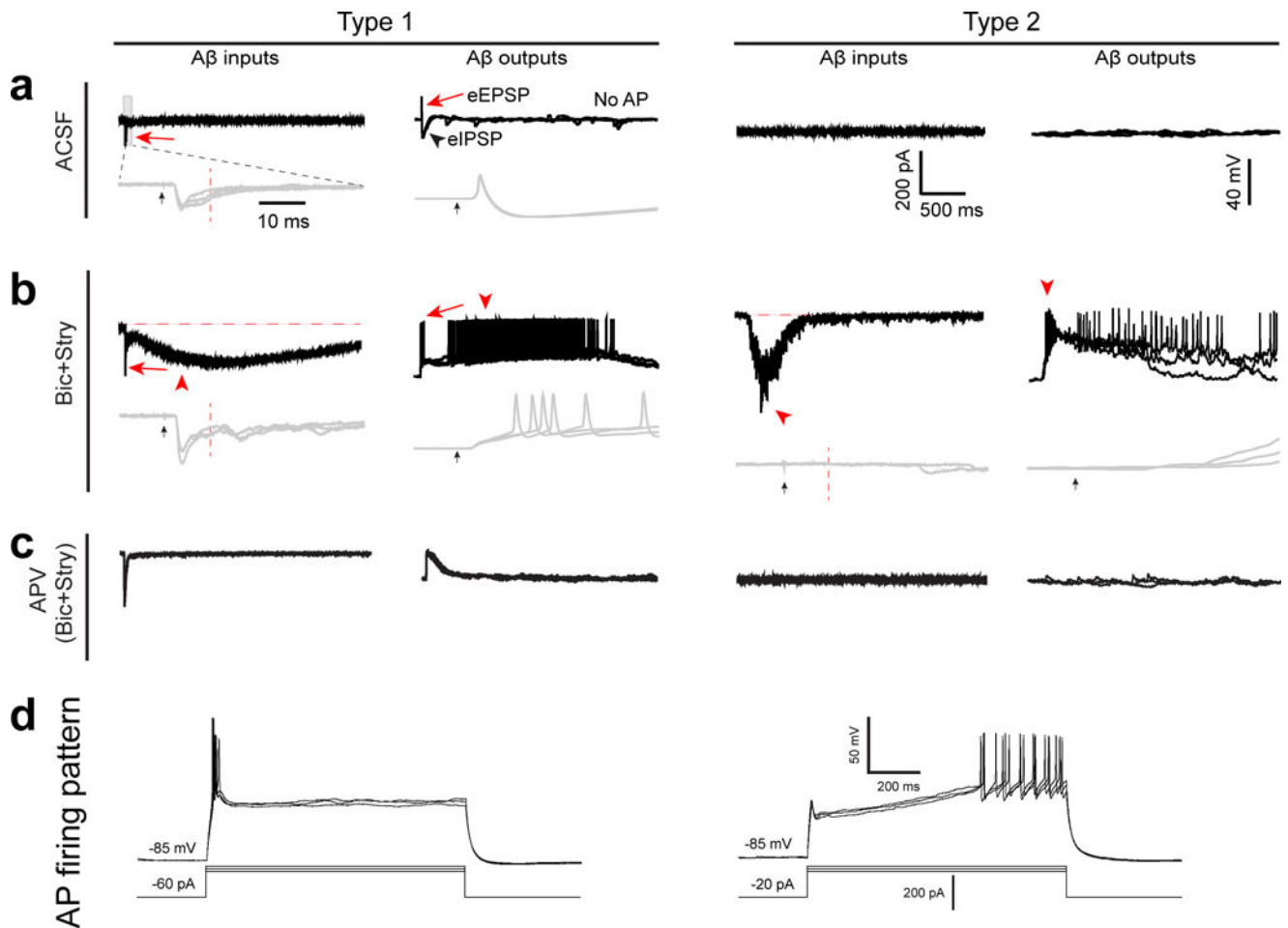
Figure 5.
Characterization of type1 and type 2 VT3^{Cre}-tdTomato$^+$ neurons. (**a,b**) Low threshold Aβ intensity stimulation-induced-inputs/outputs in type 1 and type 2 VT3^{Cre}-tdTomato$^+$ neurons before (**a**) and after (**b**) treatment with bicuculline (10 μM) plus strychnine (2 μM). The light gray traces are higher magnifications of the portions of the top black traces marked with the rectangle bar (only shown in the first panel). For type 1 neurons, with the presence of bicuculline and strychnine ("Bic+Stry"), Aβ intensity stimulation evoked both fast-onset (red arrows) and slow-onset (red arrowheads) currents with AP firing. Type 2 neurons (right panel) received slow Aβ inputs only with bicuculline and strychnine. (**c**) Bath application of NMDAR antagonist APV (50 μM) blocked slow-onset long-lasting Aβ-evoked currents and AP firing induced by bicuculline and strychnine. Black arrows indicate stimulation artifacts, red vertical dashed lines indicate the 10-ms time point following stimulation, and red horizontal dashed lines indicate baseline. (**d**) Predominant AP firing patterns of type1 and type 2 VT3^{Cre}-tdTomato$^+$ neurons, respectively. All recordings are composed of three repeated traces.
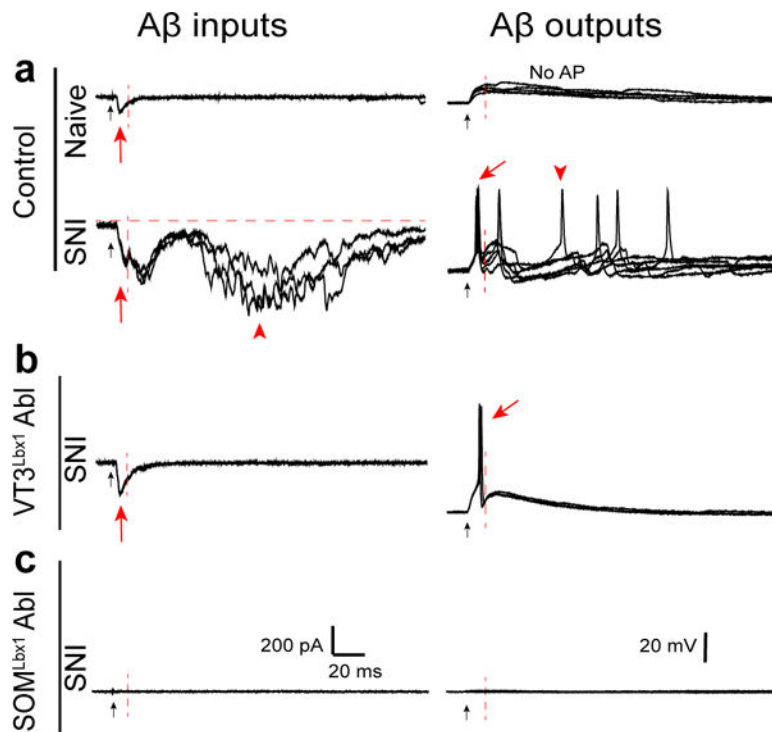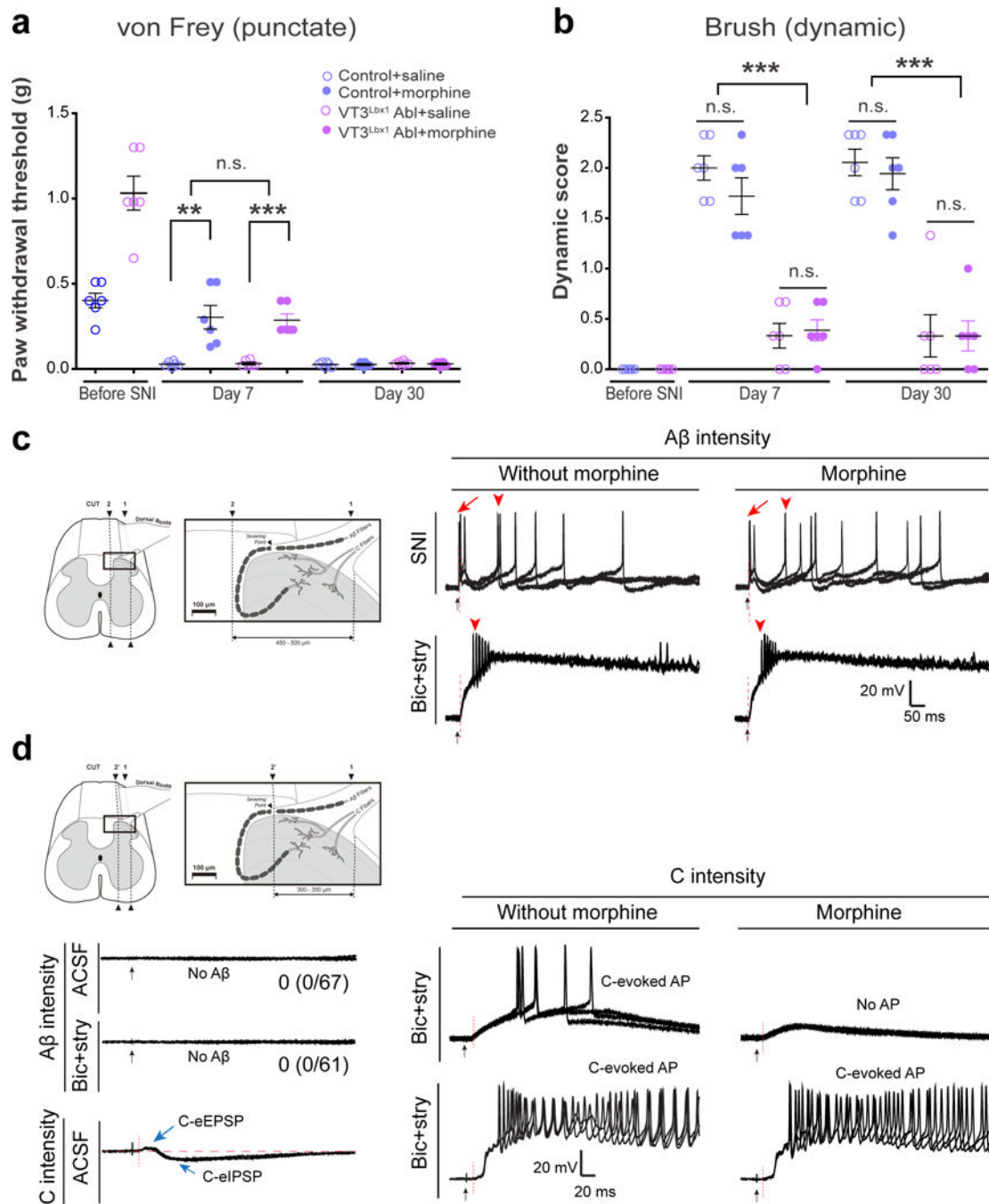
Figure 6.
Slow-onset and fast-onset Aβ pathways opened by nerve injury and mediated differentially via $VT3^{Lbx1}$ and SOM^{Lbx1} neurons. (**a-c**) Low threshold Aβ intensity-evoked-inputs/outputs in spinal $I-II_o$ neurons in control, $VT3^{Lbx1}$-neuron-ablated mice ("$VT3^{Lbx1}$ Abl") and SOM^{Lbx1}-neuron-ablated mice ("SOM^{Lbx1} Abl"), with spared nerve injury ("SNI") or without ("naïve"). Left: Aβ inputs tested by Aβ-eEPSCs at −70 mV; Right: Aβ outputs tested by Aβ-evoked EPSPs/APs at resting membrane potentials. Black arrows indicate stimulation artifacts, red vertical dashed lines indicate the 10-ms time point following stimulation, and red horizontal dashed lines indicate baseline. All recordings are composed of three repeated traces.

Figure 7.
Differential morphine sensitivity of spinal pathways. (**a,b**) Effects on punctate and dynamic hypersensitivity by intrathecal injection of morphine or saline (n = 6 in each group). In (**a**), morphine attenuated punctate hypersensitivity at day 7 post SNI in both control and ablation ("VT3[Lbx1] Abl") mice (two-way ANOVA, $F_{1, 10} = 47$, $P < 0.001$) and the degrees of inhibition are no different (two-way ANOVA, $F_{1, 10} = 0.0691$, $P = 0.798$). Morphine had no inhibitory effect at day 30 (two-way ANOVA, $F_{1, 10} = 0.237$, $P = 0.637$). In (**b**), morphine did not affect dynamic hypersensitivity in either wild type or VT3[Lbx1] Abl mice (two-way

ANOVA, Day 7: $F_{1, 10} = 1.403$, $P = 0.264$; Day 30: $F_{1, 10} = 0.366$, $P = 0.558$). Note that dynamic hypersensitivity was attenuated in VT3$^{\text{Lbx1}}$ neuron-ablated mice in comparison with control at either time point (two-way ANOVA; Day 7: $F_{1, 10} = 81.824$, $P < 0.001$; Day 30: $F_{1, 10} = 60.324$, $P < 0.001$). Data are represented as mean ± SEM. **(c)** Left panel: schematics illustration of sagittal spinal cord slice preparations to preserve electrically low-threshold Aβ-fiber inputs. Right panel: morphine resistance of Aβ-evoked AP outputs in slice from mice with SNI or with bicuculline plus strychnine ("Bic+Stry"). Red lines indicate the 10-ms time point following stimulation. Black arrows indicate stimulation artifact. Red arrows and arrowheads indicate fast-onset and slow-onset Aβ-evoked APs, respectively. **(d)** Left panel: in this "C input" preparation, electrically low-threshold Aβ inputs to VT3$^{\text{Cre}}$-tdTomato-negative $_\text{v}\text{II}_\text{i}$ neurons were absent (left, top two traces). C intensity stimulation-evoked EPSPs and IPSPs without APs (left, bottom trace). Right panel: C intensity stimulation-generated APs outputs with Bic+Stry (**d**, right panel, "Control") in VT3$^{\text{Cre}}$-tdTomato-negative neurons in $_\text{v}\text{II}_\text{i}$, which were either sensitive or resistant to morphine treatment. All recordings are composed of three repeated traces.
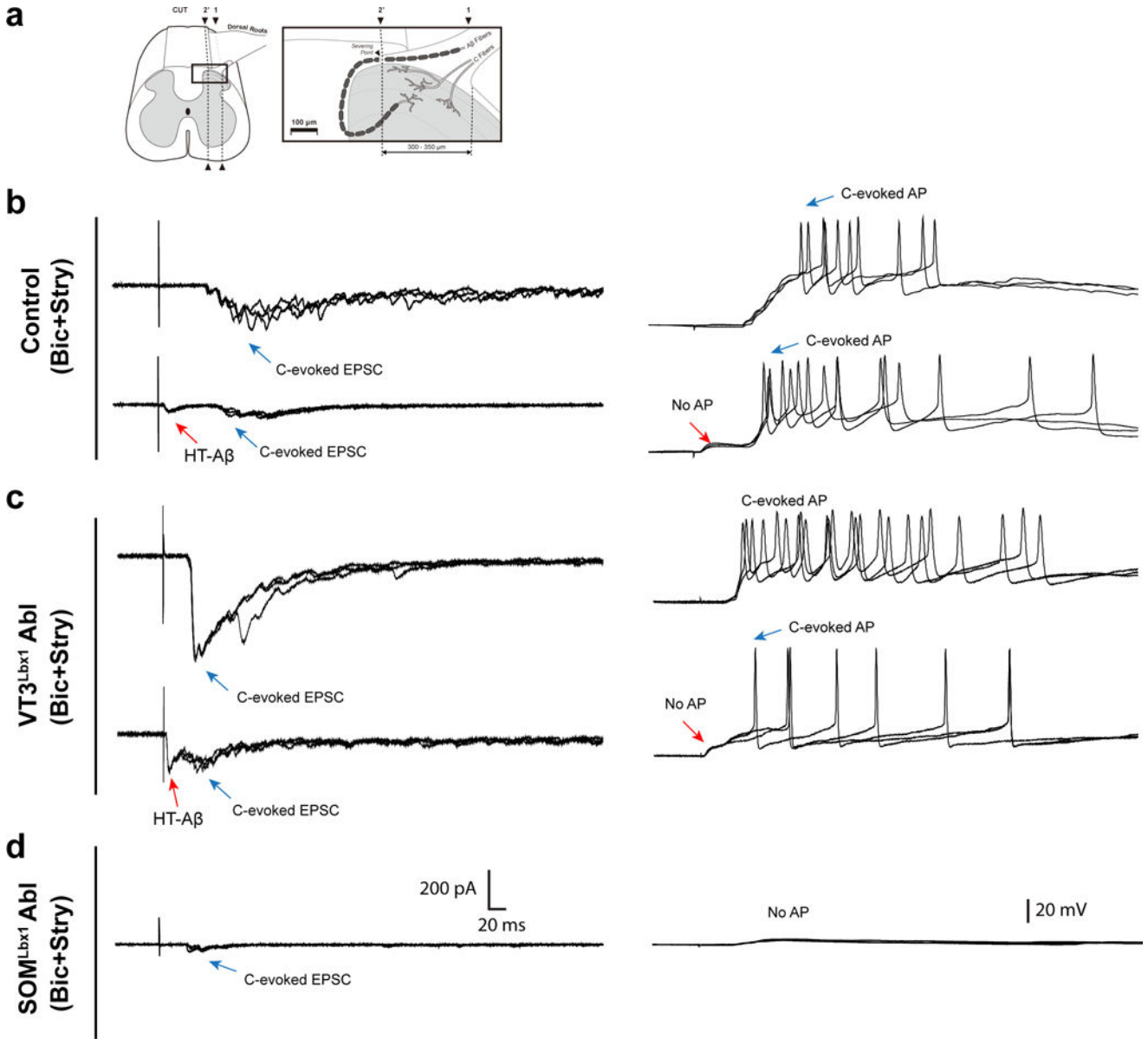
Figure 8.
Loss of C-fiber inputs to $_V$II$_i$ neurons in SOM^{Lbx1} neuron-ablated mice ("SOM^{Lbx1} Abl"), but not in VT3^{Lbx1} neuron-ablated mice ("VT3^{Lbx1} Abl"). **(a)** Schematics showing sagittal spinal cord slice preparations that removed low-threshold Aβ-fiber inputs to dorsal horn neurons. **(b–d)** C intensity stimulation-induced-inputs/outputs in $_V$II$_i$ neurons in control, SOM^{Lbx1} Abl and VT3^{Lbx1} Abl mice. Blue and red arrows indicate C fiber inputs and electrically high threshold ("HT") Aβ inputs/outputs, respectively. Typical traces shown are representative responses of 23, 37 and 20 neurons, respectively, in control, SOM^{Lbx1} Abl, and VT3^{Lbx1} Abl mice. All recordings are composed of three repeated traces.